

1  
2  
3  
4  
5  
6  
7 **Air quality and health benefits from ultra-low emission**  
8 **control policy indicated by continuous emission monitoring:**  
9 **A case study in the Yangtze River Delta region, China**  
10

11 | Yan Zhang<sup>1,2</sup>, Yu Zhao<sup>1,3\*</sup>, Meng Gao<sup>4</sup>, Xin Bo<sup>5</sup>, Chris P. Nielsen<sup>6</sup>  
12

13 | 1. State Key Laboratory of Pollution Control and Resource Reuse and School of the  
14 | Environment, Nanjing University, 163 Xianlin Rd., Nanjing, Jiangsu 210023, China.

15 | 2. Jiangsu Environmental Engineering and Technology Co., Ltd, Jiangsu  
16 | Environmental Protection Group Co., Ltd., 8 East Jialingjiang St, Nanjing, Jiangsu  
17 | 210019, China

18 | 3. Jiangsu Collaborative Innovation Center of Atmospheric Environment and  
19 | Equipment Technology (CICAEET), Nanjing University of Information Science and  
20 | Technology, Jiangsu 210044, China.

21 | 4. Department of Geography, State Key Laboratory of Environmental and Biological  
22 | Analysis, Hong Kong Baptist University, Hong Kong SAR, China.

23 | 5. The Appraisal Center for Environment and Engineering, Ministry of Environmental  
24 | Protection, Beijing 100012, China.

25 | 6. Harvard-China Project on Energy, Economy and Environment, John A. Paulson  
26 | School of Engineering and Applied Sciences, Harvard University, 29 Oxford St,  
27 | Cambridge, MA 02138, USA.  
28  
29

30 | \*Corresponding author: Yu Zhao

31 | Phone: 86-25-89680650; email: [yuzhao@nju.edu.cn](mailto:yuzhao@nju.edu.cn)  
32

删除的内容: 2

删除的内容: 3

删除的内容: 4

删除的内容: 5

删除的内容:

删除的内容: Ave

删除的内容: 2

删除的内容: 3

删除的内容: 4

删除的内容: 5

## 43 Abstract

44 To evaluate the improved emission estimates from online monitoring, we applied the  
45 Models-3/CMAQ (Community Multi-scale Air Quality) system to simulate the air  
46 quality of the Yangtze River Delta (YRD) region using two emission inventories  
47 without/with incorporated data from continuous emission monitoring systems (CEMS)  
48 at coal-fired power plants (Cases 1 and 2), respectively. The normalized mean biases  
49 (NMBs) between the observed and simulated hourly concentrations of SO<sub>2</sub>, NO<sub>2</sub>, O<sub>3</sub>  
50 and PM<sub>2.5</sub> in Case 2 were -3.1%, 56.3%, -19.5% and -1.4%, all smaller in absolute  
51 value than those in Case 1, at 8.2%, 68.9%, -24.6% and 7.6%, respectively. The  
52 results indicate that incorporation of CEMS data in the emission inventory reduced  
53 the biases between simulation and observation and could better reflect the actual  
54 sources of regional air pollution. Based on the CEMS data, the air quality changes and  
55 corresponding health impacts were quantified for different implementation levels of  
56 China's recent "ultra-low" emission policy. If the coal-fired power sector met the  
57 requirement alone (Case 3), the differences in the simulated monthly SO<sub>2</sub>, NO<sub>2</sub>, O<sub>3</sub>  
58 and PM<sub>2.5</sub> concentrations compared to those of Case 2, our base case for policy  
59 comparisons, were less than 7% for all pollutants. The result implies a minor benefit  
60 of ultra-low emission control if implemented in the power sector alone, attributed to  
61 its limited contribution to the total emissions in the YRD after years of pollution  
62 control (11%, 7% and 2% of SO<sub>2</sub>, NO<sub>x</sub> and primary particle matter (PM) in Case 2,  
63 respectively). If the ultra-low emission policy was enacted at both power plants and  
64 selected industrial sources including boilers, cement, and iron & steel factories (Case  
65 4), the simulated SO<sub>2</sub>, NO<sub>2</sub> and PM<sub>2.5</sub> concentrations compared to the base case were  
66 33%-64%, 16%-23% and 6%-22% lower respectively, depending on the month  
67 (January, April, July and October 2015). Combining CMAQ and the Integrated  
68 Exposure Response (IER) model, we further estimated that 305 deaths and 8744 years  
69 of life loss (YLL) attributable to PM<sub>2.5</sub> exposure could be avoided with the  
70 implementation of the ultra-low emission policy in the power sector in the YRD  
71 region. The analogous values would be much higher, at 10,651 deaths and 316,562  
72 YLL avoided, if both power and industrial sectors met the ultra-low emission limits.  
73 In order to improve regional air quality and to reduce human health risk effectively,  
74 coordinated control of multiple sources should be implemented, and the ultra-low

删除的内容: estimation

删除的内容: data

带格式的: 缩进: 首行缩进: 0 厘米

删除的内容: of annual SO<sub>2</sub>, NO<sub>2</sub>, O<sub>3</sub> and PM<sub>2.5</sub> concentrations

删除的内容: observations

删除的内容: simulations

删除的内容: helped

删除的内容: can

删除的内容: only

删除的内容: simulated

删除的内容: only

删除的内容: in the sector

删除的内容:

删除的内容: , accounting for 5.5% and 6.2% of the totals for the region, respectively.

删除的内容: various pollution

92 | emission policy should be substantially expanded to major emission sources in  
93 non-power industries.

刪除的內容: control

刪除的內容: industrial boilers and

刪除的內容: other

## 94 1. Introduction

95 Due to swift economic development and associated growth in demand for  
96 electricity, coal-fired power plants have played an important role in energy  
97 consumption and air pollutant emissions for a long time in China. For example, Zhao  
98 et al. (2008) for the first time developed a “unit-based” emission inventory of primary  
99 air pollutants from the coal-fired power sector in China and found that the sector  
100 contributed 53% and 36% to the national total emissions of SO<sub>2</sub> and NO<sub>x</sub>,  
101 respectively, in 2005. Subsequently, SO<sub>2</sub> and NO<sub>x</sub> emissions from the power sector  
102 were estimated to account respectively for 28%-53% and 29%-31% of the total annual  
103 emissions in China during 2006-2010 according to the Multi-resolution Emission  
104 Inventory for China (MEIC: <http://www.meicmodel.org>). To reduce high emissions  
105 and improve air quality in China, advanced air pollutant control devices (APCDs)  
106 have been gradually applied in the power sector including flue gas desulfurization  
107 (FGD) for SO<sub>2</sub> control, selective catalytic reduction (SCR) for NO<sub>x</sub> control, and  
108 high-efficiency dust collectors for primary particulate matter (PM) control. In recent  
109 years, moreover, an “ultra-low emission” retrofitting policy has been widely  
110 implemented, seeking to reduce the emission levels of coal-fired power plants to those  
111 of gas-fired ones (i.e., 35, 50, and 5 mg/m<sup>3</sup> for SO<sub>2</sub>, NO<sub>x</sub> and PM concentrations in  
112 the flue gas). The expanded use of associated technologies has induced great changes  
113 in the magnitude and spatio-temporal distribution of emissions from the power sector,  
114 which have been analyzed and quantified by a series of studies (Y. Zhao et al., 2013;  
115 Zhang et al., 2018; Liu et al., 2019; Tang et al., 2019; Y. Zhang et al., 2019). With the  
116 updated unit-level information, for example, MEIC estimated that the power sector  
117 shares of national total emissions declined from 28% to 22% and from 29% to 21%  
118 for SO<sub>2</sub> and NO<sub>x</sub> during 2010-2015, respectively. Incorporating data from continuous  
119 emission monitoring systems (CEMS), Tang et al. (2019) found that China’s annual  
120 power sector emissions of SO<sub>2</sub>, NO<sub>x</sub> and PM declined by 65%, 60% and 72%  
121 respectively during 2014-2017, due to the enhanced control measures. With a method  
122 of collecting, examining and applying CEMS data, similarly, our previous work  
123 indicated that the estimated emissions from the power sector would be 75%, 63% and

127 76% smaller than those calculated without CEMS data for SO<sub>2</sub>, NO<sub>x</sub> and PM,  
128 respectively (Y. Zhang et al., 2019).

129 Evaluations of emission estimates and the changed air quality from emission  
130 abatement provide useful information on the sources of air pollution and the  
131 effectiveness of pollution control measures. Air quality modeling is an important tool  
132 for evaluating emission inventories, by comparing simulation results with available  
133 observation data. Developed by the U.S. Environmental Protection Agency (USEPA),  
134 the Models-3/Community Multi-scale Air Quality (CMAQ) system has been widely  
135 used in China (Li et al., 2012; An et al., 2013; Wang et al., 2014; Han et al., 2015;  
136 Zheng et al., 2017; Zhou et al., 2017; Chang et al., 2019). Han et al. (2015) conducted  
137 CMAQ simulations with different emission inventories for East Asia, and found that  
138 the simulated NO<sub>2</sub> columns using the emission inventory for the Intercontinental  
139 Chemical Transport Experiment-Phase B (INTEX-B, Zhang et al., 2009) agreed better  
140 with the satellite observations of the Ozone Monitoring Instrument (OMI) than the  
141 simulations using the Regional Emission Inventory in Asia (REAS v1.11, Ohara et al.,  
142 2007). Zhou et al. (2017) applied CMAQ to evaluate the national, regional and  
143 provincial emission inventories for the Yangtze River Delta (YRD) region, and the  
144 best model performance with the provincial inventory confirmed that the emission  
145 estimate with more detailed information incorporated on individual power and  
146 industrial plants helped improve the air quality simulation at relatively high horizontal  
147 resolution. With air quality modeling, moreover, many studies have explored the  
148 environment benefits of emission control measures taken in recent years (B. Zhao et  
149 al., 2013; Huang et al., 2014; Li et al., 2015; Wang et al., 2015; Tan et al., 2017).  
150 Wang et al. (2015) found that the implementation of the new Emission Standard of Air  
151 Pollutants for Thermal Power Plants (GB13223-2011) could effectively reduce  
152 pollutant emissions in China, and the **ambient** concentrations of SO<sub>2</sub>, NO<sub>2</sub> and PM<sub>2.5</sub>  
153 would decrease by 31.6%, 24.3% and 14.7% respectively in 2020 compared with a  
154 baseline scenario for 2010. Li et al. (2015) found that the simulated concentrations of  
155 PM<sub>2.5</sub> in the YRD region would decrease by 8.7%, 15.9% and 24.3% from 2013 to  
156 2017 in three scenarios with weak, moderate and strong emission reduction  
157 assumptions in the Clean Air Action Plan, respectively.

158 Besides air quality, the health risk caused by air pollution exposures in China is a  
159 major concern, especially to PM<sub>2.5</sub>, a dominant pollutant in haze conditions. Lim et al.

删除的内容: environmental

删除的内容: itself

162 (2012) has identified air pollution as a primary cause of global burden of disease,  
163 especially in low- and middle-income countries, and PM<sub>2.5</sub> pollution was ranked the  
164 fourth leading cause of death in China. Studies have shown that PM<sub>2.5</sub> is closely  
165 related to several causes of death (Dockery et al., 1993; Hoek et al., 2013; Lelieveld et  
166 al., 2015; Butt et al., 2017; Gao et al., 2018; Maji et al., 2018; Hong et al., 2019). For  
167 example, Lelieveld et al. (2015) estimated that nearly 1.4 million people died each  
168 year due to PM<sub>2.5</sub> exposure in China, 18% of which were related to the emissions from  
169 the power sector. Based on simulated PM<sub>2.5</sub> using WRF-Chem and the Integrated  
170 Exposure Response (IER) model, Gao et al. (2018) estimated that emissions from the  
171 power sector results in 15 million years of life lost per year in China. In addition to  
172 assessment of health risk based on observations of actual air pollution levels, studies  
173 have also analyzed the health benefits of emission control policies (Lei et al., 2015; Li  
174 and Li, 2018; Dai et al., 2019; Q. Zhang et al., 2019; X. Zhang et al., 2019).  
175 Combining available observation and CMAQ modeling, Q. Zhang et al. (2019)  
176 identified improved emission controls on industrial and residential pollution sources  
177 as the main drivers of reductions in PM<sub>2.5</sub> concentrations from 2013 to 2017 in China,  
178 and estimated an annual reduction of PM<sub>2.5</sub>-related deaths at 0.41 million. Lei et al.  
179 (2015) evaluated the health benefit of the Air Pollution Prevention and Control Action  
180 Plan of China, and found that full realization of the air quality goal in this plan could  
181 avoid 89 thousand premature deaths of urban residents, and reduce 120,000 inpatient  
182 cases and 9.4 million outpatient service and emergency cases. Focusing more  
183 regionally, X. Zhang et al. (2019) estimated the health impact of a "coal-to-electricity"  
184 policy for residential energy use in the Beijing-Tianjin-Hebei (BTH) region. They  
185 projected that the reduction in PM<sub>2.5</sub> concentrations from the policy would avoid  
186 nearly 22,200 cases of premature death and 607,800 cases of disease in the region in  
187 2020. For areas with strong, industry-based economies, the impact of air quality on  
188 public health can be more significant, attributed both to relatively large and dense  
189 populations and to high pollution levels. Until now, however, there have been few  
190 studies focusing on air quality improvement and corresponding health benefits  
191 attributed to the implementation of the latest emission control policies, notably  
192 China's ultra-low emission policy introduced above, at regional scale.

193 As one of the most densely populated and economically developed regions, the  
194 YRD region encompassing Shanghai and Anhui, Jiangsu, and Zhejiang provinces is a

195 key area for air pollution prevention and control in China (Huang et al., 2011; Li et al.,  
196 2011; Li et al., 2012). It is also one of the regions with the earliest implementation of  
197 the ultra-low emission policy on the power sector in the country. Quantification of  
198 emission reductions and subsequent changes in air quality is crucial for full  
199 understanding of the environmental benefits of the policy. To test the possible  
200 improvement in the regional emission inventory, this study evaluated the air quality  
201 modeling performance without and with CEMS data incorporated in the estimation of  
202 emissions of the coal-fired power sector for the YRD region. The changes in regional  
203 air quality and health risk resulting from the implementation of the ultra-low emission  
204 policy for key industries were quantified combining the air quality modeling and the  
205 health risk model. The results provide scientific support for incorporation of online  
206 monitoring data to improve the estimation of air pollutant emissions, and for better  
207 design of emission control policies based on their simulated environmental effects.  
208

## 209 **2. Methodology and data**

### 210 **2.1 Air quality modeling**

211 In this study, we adopted CMAQ version 4.7.1 (UNC, 2010) to conduct air  
212 quality simulations and to evaluate various emission inventories for the YRD region.  
213 The model has performed well in Asia (Zhang et al., 2006; Uno et al., 2007; Fu et al.,  
214 2008; Wang et al., 2009). Two one-way nested domains were adopted for the  
215 simulations, and the horizontal resolutions were set at 27 and 9 km square grid cells  
216 respectively, as shown in Figure 1. The mother domain (D1,  $177 \times 127$  cells) covered  
217 most of China and all or parts of surrounding countries in East, Southeast, and South  
218 Asia. The second modeling region (D2,  $118 \times 121$  cells) covered the YRD region,  
219 including Jiangsu, Zhejiang, Shanghai, Anhui and parts of surrounding provinces.  
220 Lambert Conformal Conic Projection was applied for the entire simulation area  
221 centered at ( $110^\circ\text{E}$ ,  $34^\circ\text{N}$ ) with two true latitudes,  $40^\circ\text{N}$  and  $25^\circ\text{N}$ . The simulated  
222 periods were January, April, July and October 2015, as representative of the four  
223 seasons. The first five days in each month were set as a spin-up period to provide  
224 initial conditions for later simulations. The carbon bond gas-phase mechanism (CB05)  
225 and AERO5 aerosol module were adopted in all the CMAQ modules, with details of

226 the model configuration found in Zhou et al. (2017). The initial concentrations and  
227 boundary conditions for the D1 mother domain were the default clean profile, while  
228 they were extracted from CMAQ outputs of D1 simulations for the nested D2 domain.  
229 Normalized mean bias (NMB), normalized mean error (NME), and the correlation  
230 coefficient (R) between the simulations and observations were selected to evaluate the  
231 performance of CMAQ modeling (Yu et al., 2006). The hourly concentrations of SO<sub>2</sub>,  
232 NO<sub>2</sub>, O<sub>3</sub> and PM<sub>2.5</sub> were observed at 230 state-operated ground stations of the national  
233 monitoring network in the YRD region and were collected from Qingyue Open  
234 Environmental Data Center (<https://data.epmap.org>).

235 The Weather Research and Forecasting (WRF) Model version 3.4  
236 (<http://www.wrf-model.org/index.php>, Skamarock et al., 2008) was applied to provide  
237 meteorological fields for CMAQ. Terrain and land-use data were taken from global  
238 data of the U.S. Geological Survey (USGS), and the first-guess fields of  
239 meteorological modeling were obtained from the final operational global analysis data  
240 (ds083.2) by the National Center for Environmental Prediction (NCEP). Statistical  
241 indicators including bias, index of agreement (IOA), and root mean squared error  
242 (RMSE) were chosen to evaluate the performance of WRF modeling against  
243 observations (Baker et al., 2004; Zhang et al., 2006). Ground observations at 3-h  
244 intervals of four meteorological parameters including temperature at 2 m (T2),  
245 relative humidity at 2 m (RH2), and wind speed and direction at 10 m (WS10 and  
246 WD10) of 42 surface meteorological stations in the YRD region were downloaded  
247 from the National Climatic Data Center (NCDC). The statistical indicators for WS10,  
248 WD10, T2 and RH2 in the YRD region are summarized by month in Table S1 in the  
249 Supplement. The discrepancies between WRF simulations and observations of these  
250 meteorological parameters were generally acceptable (Emery et al., 2001). Better  
251 agreements were found for T2 and RH2 with their biases ranging -0.62 to +0.12°C  
252 and -3.20% to +6.60% respectively, and their IOAs were all within the benchmarks  
253 (Emery et al., 2001). In general, WRF captured well the characteristics of main  
254 meteorological conditions for the region.

## 255 **2.2 Emission inventories and cases**

256 The anthropogenic emissions from industry, residential and transportation sectors  
257 for D1 and D2 were obtained from the national emission inventory developed in our

258 previous work (Xia et al., 2016). The total emissions excluding those of the power  
259 sector of SO<sub>2</sub>, NO<sub>x</sub> and PM for the YRD region were estimated at 1501.0, 3468.4 and  
260 2711.2 Gg for 2015, respectively. The emission inventory in Xia et al. (2016) was  
261 developed using activity data at the provincial level, and the spatial distribution of  
262 emissions by sector was conducted according to that of MEIC with the original spatial  
263 resolution of 0.25° × 0.25° in this study. The gridded emissions were further  
264 downscaled to horizontal resolutions of 27 and 9 km in D1 and D2, respectively,  
265 based on the spatial distribution of population (for residential sources), industrial  
266 gross domestic product (for industrial sources), and the road network (for on-road  
267 vehicles). The monthly variations of emissions from each sector were assumed to be  
268 the same as in MEIC. Constrained by available ground observation, a larger monthly  
269 variation in the emissions of black carbon aerosols was found for the central YRD  
270 region than that in MEIC. Limited improvement in air quality model performance was  
271 consequently achieved, implying that the bias from the temporal variation was  
272 insignificant (Zhao et al., 2019). In addition, the Model Emissions of Gases and  
273 Aerosols from Nature developed under the Monitoring Atmospheric Composition and  
274 Climate project (MEGAN-MACC, Guenther et al., 2012; Sindelarova et al., 2014)  
275 were applied as the biogenic emission inventory, and the emissions of Cl, HCl and  
276 lightning NO<sub>x</sub> were obtained from the Global Emissions Initiative (GEIA, Price et al.,  
277 1997).

删除的内容: s

278 For the power sector in the YRD region specifically, we adopted the unit-level  
279 emission estimates from our previous study and allocated the emissions according to  
280 the actual locations of individual units (Y. Zhang et al., 2019). As described in that  
281 study, the detailed information at the power unit level was compiled based on official  
282 environmental statistics including the geographic location, installed capacity, fossil  
283 fuel consumption, combustion technology, and APCDs. Besides the commonly used  
284 method, Y. Zhang et al. (2019) developed a new method of examining, screening and  
285 applying CEMS data to improve the estimates of power sector emissions. CEMS data  
286 were collected for over 1000 power units, including operation condition, monitoring  
287 time, flue gas flow, and hourly concentrations of SO<sub>2</sub>, NO<sub>x</sub> and PM. The emissions of  
288 individual unit were calculated based on the hourly concentrations of air pollutants  
289 obtained from CEMS and the theoretical flue gas volume estimated based on the  
290 unit-level information mentioned above. Compared to MEIC, a larger monthly

删除的内容: the

删除的内容: The geographic locations of power units were taken initially from the environmental statistics, and then adjusted using Google Earth.



298 variation in emissions was found based on the online emission monitoring. More  
299 details can be found in Y. Zhang et al. (2019). In this work, five emission cases were  
300 set for the air quality simulation. Cases 1 and 2 used estimates of power sector  
301 emissions without/with incorporation of CEMS data, and were compared against each  
302 other to evaluate the benefit of online emission monitoring information in air quality  
303 simulation. Note Case 2 was set as the base case for further analysis of the effects of  
304 emission controls. Based on the unit-level information from CEMS, Case 3, assumed  
305 that only power plants would meet the requirement of the ultra-low emission policy,  
306 while Case 4 assumed both power plants and selected industrial sources including  
307 boilers, cement, and iron & steel factories would meet the requirement. As  
308 summarized in Table S2 in the supplement, the ultra-low emission limits for the flue  
309 gas concentrations were obtained from the most recent national or local standards by  
310 sector (Yang et al., 2021). The model performances were compared with the base case  
311 to quantify the air quality improvements that result from the policy. Case 5 removed  
312 all the emissions from the power sector and thus helped to specify the contribution of  
313 the power sector to air pollution in the YRD region.

删除的内容: As shown in in Table 1, i

删除的内容: n total

删除的内容: s

删除的内容: and 4 calculated emissions

删除的内容: assuming

删除的内容: boilers, or both power plant and industrial boilers

删除的内容: s

删除的内容: respectively

314 The air pollutant emissions for all the cases are summarized by sector in Table 1.  
315 With the CEMS data for the power sector incorporated, the total emissions of SO<sub>2</sub>,  
316 NO<sub>x</sub> and PM for the YRD region in Case 2 were estimated as 427, 618 and 331 Gg  
317 smaller than those in Case 1, with relative reductions of 20%, 14% and 11%  
318 respectively. Benefiting from the implementation of the ultra-low emission policy in  
319 the coal-fired power sector, the total emissions of anthropogenic SO<sub>2</sub>, NO<sub>x</sub> and PM in  
320 Case 3 would further decline 123, 135 and 36 Gg compared to Case 2, respectively.  
321 The analogous numbers for Case 4 were 1180, 1003, and 1315 Gg, and the reduction  
322 rates compared to Case 2 were 70%, 27%, and 48% for SO<sub>2</sub>, NO<sub>x</sub> and PM,  
323 respectively. The implementation of the ultra-low emission policy for both power and  
324 industry sectors would significantly reduce the primary pollutant emissions for the  
325 YRD region. In Case 5 where the emissions from power sector were set as zero, the  
326 total emissions of SO<sub>2</sub>, NO<sub>x</sub> and PM were estimated to decrease by 11%, 7% and 2%  
327 respectively compared to Case 2.

删除的内容:

删除的内容: S2 in the Supplement

### 328 2.3 Health effect analysis

329 We applied the IER model of the Global Burden of Disease Study (GBD) 2015

342 (Cohen et al., 2017) and quantified the impact of emission control policy on the  
 343 human health risk due to long-term exposure of PM<sub>2.5</sub> in the YRD region. The model  
 344 has been well developed and widely applied in quantifying the impact of air pollution  
 345 control policies on health burden (Li et al. 2019; Yue et al. 2020; Zheng et al. 2019).  
 346 Compared to another widely used model Global Exposure Mortality Model (GEMM;  
 347 Burnett et al., 2018), IER was expected to provide relatively conservative estimates  
 348 for China (Yang et al., 2021). The number of attributable deaths and years of life lost  
 349 (YLL) caused by long-term PM<sub>2.5</sub> exposure for selected emission cases were  
 350 calculated for various diseases in this study. In particular, YLL represents the years of  
 351 life lost because of premature death from a particular cause or disease. As the number  
 352 of deaths alone could not provide a comprehensive picture of the burden that deaths  
 353 impose on the population, we calculated YLL caused by PM<sub>2.5</sub> exposure to help  
 354 describe the extent to which the lives of people exposed to air pollution were cut short.  
 355 We considered the four adult diseases of the GBD study, including ischemic heart  
 356 disease (IHD), stroke (STK, including ischemic and hemorrhagic stroke), lung cancer  
 357 (LC), and chronic obstructive pulmonary disease (COPD), and a common disease  
 358 among young children, acute lower respiratory infection (LRI).

删除的内容:

删除的内容: five

删除的内容: It

359 The health risks in the different emission cases were estimated following Gao et  
 360 al. (2018) with the updated information for 2015. First, the relative risk (RR) for each  
 361 disease was calculated using eq. (1):

$$362 \quad RR_{i,j,k}(Cl) = \begin{cases} 1 + \partial_{i,j,k}(1 - e^{-\beta_{i,j,k}(Cl-C_0)^{\gamma_{i,j,k}}}), & Cl \geq C_0 \\ 1, & Cl < C_0 \end{cases} \quad (1)$$

363 where  $i$ ,  $j$ , and  $k$  represent the age, gender and disease type, respectively;  $Cl$  is the  
 364 annual average PM<sub>2.5</sub> concentration simulated with WRF-CMAQ (the average of  
 365 January, April, July and October in this work);  $C_0$  is the counterfactual concentration;  
 366 and  $\partial$ ,  $\beta$  and  $\gamma$  are the parameters that describe the IER functions, as reported by  
 367 Cohen et al. (2017).

368 Secondly, the population attributable fractions (PAF) were calculated with RR  
 369 following eq. (2) by disease, age and gender subgroup:

$$370 \quad PAF_{i,j,k} = \frac{RR_{i,j,k}(Cl) - 1}{RR_{i,j,k}(Cl)} \quad (2)$$

371 Moreover, the mortality attributable to PM<sub>2.5</sub> exposure ( $\Delta M$ ) was calculated  
 372 using eq. (3), where  $y_0$  is the current age-gender-specific mortality rate, and  $Pop$

376 | represents the exposed population in the age-gender-specific group in grid cell  $l$ :

$$377 \quad \Delta M_{i,j,k,l} = PAF_{i,j,k,l} \times \gamma_{oi,j,k,l} \times Pop_{i,j,l} \quad (3)$$

378 | The population data of the four provinces and cities in the YRD region were  
379 | obtained from statistical yearbooks (AHBS, 2016; JSBS, 2016; SHBS, 2016; ZJBS,  
380 | 2016), and the gender distribution by province is shown in Table S3 in the  
381 | Supplement. As the high-resolution spatial pattern of age structure was unavailable,  
382 | we assumed the same age structure for all the model grids according to Gao et al.  
383 | (2018). The baseline age-gender-disease-specific mortality rates for the five diseases  
384 | in China for 2015 were obtained from the Global Health Data Exchange database  
385 | (GHDx, <https://vizhub.healthdata.org>), as shown in Table S4 in the Supplement, and  
386 | those by province were calculated based on the provincial proportions in Xie et al.  
387 | (2016). The national population with the spatial resolution at 1×1 km in 2015 was  
388 | provided by the Landscan Global Demographic Dynamic Analysis Database  
389 | developed by Oak Ridge National Laboratory (ORNL) of the U.S. Department of  
390 | Energy. As shown in Figure S1 in the Supplement, the population densities in the  
391 | YRD region are larger in Shanghai, southern Jiangsu and northern Zhejiang.

删除的内容:

392 | Finally, the year of life lost (YLL) due to PM<sub>2.5</sub> exposure was calculated from the  
393 | number of deaths multiplied by a standard life expectancy at the age at which death  
394 | occurs, as shown in eq. (4), where  $N$  represents the number of deaths in each  
395 | age-gender-specific group, and  $L$  reflects the remaining life expectancy of the group:

删除的内容: following

$$396 \quad YLL = \sum_{i,j} N_{i,j} \times L_{i,j} \quad (4)$$

397 | The remaining life expectancies by age were obtained from the life tables from  
398 | the World Health Organization (WHO, <https://www.who.int>), as summarized in Table  
399 | S5 in the Supplement. The life expectancies at birth of Chinese males and females in  
400 | 2015 were 74.8 and 77.7 years, respectively.

### 401 | **3. Results and discussion**

#### 402 | **3.1 Evaluation of emission estimates with air quality simulation**

##### 403 | **3.1.1 Model performances without/with CEMS data**

404 | Air quality simulations based on emission inventories without/with incorporation  
405 | of CEMS data for the coal-fired power sector (Cases 1 and 2, respectively) were

408 conducted to test the improvement of emission estimates. Because of the combined  
409 influences of regional transport and chemical reactions of air pollutants in the  
410 atmosphere, nonlinear relationships were found between the changes of primary  
411 emissions and ambient concentrations of air pollutants. Compared to Case 1, the  
412 simulated annual average concentrations of SO<sub>2</sub>, NO<sub>2</sub> and PM<sub>2.5</sub> in the YRD region  
413 were 10%, 7% and 6% lower respectively in Case 2, while that of O<sub>3</sub> was 7% higher,  
414 due to combined effects of emissions of volatile organic compounds (VOCs) and NO<sub>x</sub>  
415 precursors (Gao et al., 2005; Yang et al., 2012). Previous studies have shown that O<sub>3</sub>  
416 formation in most of the YRD region is under the “VOCs-limited” regime, i.e., the  
417 generation and removal of O<sub>3</sub> is more sensitive to VOCs and would be inhibited with  
418 high NO<sub>x</sub> concentrations in the atmosphere (Zhang et al., 2008; Liu et al., 2010;  
419 Wang et al., 2010; Xing et al., 2011). Therefore, the simulated reduced NO<sub>2</sub>  
420 concentrations from greater NO<sub>x</sub> emission control could elevate the O<sub>3</sub> concentration.

421 The ~~model performance was evaluated with available ground observation. The~~  
422 ~~hourly concentrations were observed at 230 state-operated air quality monitoring~~  
423 ~~stations within YRD, and the averages of hourly concentrations of those sites were~~  
424 ~~compared with the simulations in Cases 1 and 2, as summarized in Table 2.~~ Similar  
425 model performances were found for the two emission cases, with overestimation of  
426 SO<sub>2</sub>, NO<sub>2</sub> and PM<sub>2.5</sub> and underestimation of O<sub>3</sub>. The NMEs between the simulated  
427 and observed SO<sub>2</sub>, O<sub>3</sub> and PM<sub>2.5</sub> concentrations were all smaller than 50% for both  
428 cases, and slightly worse simulation performances were found in July compared to the  
429 other three months. In particular, the correlation coefficients (R) between the  
430 simulated and observed SO<sub>2</sub> in July were only 0.17 and 0.14 for Cases 1 and 2,  
431 respectively, and the NMEs between the simulated and observed NO<sub>2</sub> were larger than  
432 100%. In addition, greater overestimation of SO<sub>2</sub> and PM<sub>2.5</sub> by the model was found  
433 in July than other months, likely attributable to ~~the~~ bias of WRF modeling. On one  
434 hand, the simulated WS10 in the YRD region in July (2.67 m/s) was slightly lower  
435 than the observation (2.75 m/s). The underestimation in wind speed could weaken the  
436 horizontal diffusion and lead to overestimation in air pollutant concentrations.  
437 Compared with the results from the European Centre for Medium-range Weather  
438 Forecasts (ECMWF, <https://apps.ecmwf.int/datasets>), on the other hand, the simulated  
439 boundary layer height (BLH) was lower in WRF for all months. The NMBs of the  
440 WRF and ECMWF BLH in January, April and October were around -15%, while that

删除的内容: simulated concentrations of SO<sub>2</sub>, NO<sub>2</sub>, O<sub>3</sub> and PM<sub>2.5</sub> based on the two emission inventories without/with CEMS data were compared

删除的内容: s and are summarized in Table 2

448 in July reached -24%. The lower BLH would limit the vertical convection and  
449 diffusion of pollutants, and thereby increase the surface concentrations of air  
450 pollutants. Similar to previous studies (An et al., 2013; Liao et al., 2015; Tang et al.,  
451 2015; Gao et al., 2016; Wang et al., 2016; Zhou et al., 2017), underestimation of O<sub>3</sub>  
452 was commonly found. ~~The NMBs between the simulation and observation for the two~~  
453 ~~cases ranged from -34.5% to -6.4%, and NMEs from 23.1% to 37.1%, respectively.~~  
454 The underestimation in O<sub>3</sub> likely resulted from bias in the estimation of precursor  
455 emissions. Suggested by the positive NMBs of NO<sub>2</sub> modeling in Table 2, the NO<sub>x</sub>  
456 emissions were expected to be overestimated in the two cases, even for Case 2 with  
457 the CEMS data incorporated (which reflect the emission control benefits in recent  
458 years, as discussed in Y. Zhang et al., 2019). In addition, underestimation of VOC  
459 emissions is likely due to incomplete accounting of emission sources, particularly for  
460 uncontrolled or fugitive leakage (Zhao et al, 2017). ~~As most of YRD was identified as~~  
461 ~~a VOC-limited region for O<sub>3</sub> formation (Wang et al., 2019; Yang et al., 2021),~~ the  
462 overestimation of NO<sub>x</sub> and underestimation of VOCs ~~could contribute to the~~  
463 ~~underestimation in~~ O<sub>3</sub> concentrations ~~with air quality modeling.~~ The simulations of  
464 both cases captured well the temporal variations of PM<sub>2.5</sub> concentrations, with the R  
465 between the observed and simulated concentrations around 0.9.

466 In general, better modeling performance in the YRD region was found in Case 2  
467 than Case 1. The ~~NMBs between the simulated and observed concentrations of SO<sub>2</sub>,~~  
468 ~~NO<sub>2</sub>, O<sub>3</sub> and PM<sub>2.5</sub> for the whole simulation period~~ were -3.1%, 56.3%, -19.5% and  
469 -1.4% for Case 2, smaller in absolute value than those for Case 1 at 8.2%, 68.9%,  
470 -24.6% and 7.6%, respectively. The bootstrap sampling (Gleser et al., 1996; He et al.,  
471 2017) was further applied to test the significance of the improvements of Case 2 over  
472 Case 1. (A significant difference is demonstrated if the confidence intervals of given  
473 statistical indices sampled from the two cases do not overlap.) As can be seen in Table  
474 2, the modeling performances of the concerned species in Case 2 were improved  
475 significantly in most instances compared to Case 1. For example, the improvement of  
476 NMB for the SO<sub>2</sub> simulation was significant at the 99% confidence level for July and  
477 October, and 95% for January. The improvement of NMB and NME for NO<sub>2</sub> was  
478 significant at confidence levels of 99% and 95% respectively for April. The  
479 improvement of NMB for O<sub>3</sub> was significant at the 95% confidence level for January,  
480 and that of PM<sub>2.5</sub> at 95% for April and 99% for July. The statistical test confirms that

删除的内容: , and

删除的内容: the

删除的内容: and NMEs

删除的内容: 1.6

删除的内容: and

删除的内容: 27

删除的内容: 5

带格式的: 下标

删除的内容: In a VOC-limited regime, therefore

删除的内容: would

删除的内容: lower simulated

删除的内容: than observation

删除的内容: s

删除的内容: In general, t

删除的内容: monthly average

496 incorporation of online monitoring data in the emission inventory can improve the  
497 regional air quality modeling for the YRD region. Besides the emission data, it should  
498 also be noted that the changes in model schemes would affect the model performance.  
499 For example, the newer version of CMAQ incorporated the chemistry schemes of  
500 bromine and iodine, and was expected to influence the O<sub>3</sub> simulation importantly.  
501 According to our recent test in the YRD region (Lu et al., 2020), the impact of CMAQ  
502 version on the simulation of difference species was inconclusive, implying the  
503 necessity of further intercomparison and evaluation studies for the region.

带格式的：下标

504 Figure 2 illustrates the spatial patterns of the simulated monthly SO<sub>2</sub>, NO<sub>2</sub>, O<sub>3</sub>  
505 and PM<sub>2.5</sub> concentrations for Case 2. For a given species, similar patterns were found  
506 for different months. In general, the simulated concentrations of SO<sub>2</sub>, NO<sub>2</sub> and PM<sub>2.5</sub>  
507 were larger in central and northern Anhui, southern Jiangsu, Shanghai and coastal  
508 areas in Zhejiang, where large power and industrial plants are concentrated, as shown  
509 in Figure S2 in the Supplement. In the highly populated cities (Shanghai, Nanjing,  
510 Hangzhou, and Hefei; see their locations in Figure 1), the simulated concentrations of  
511 pollutants were significantly larger than their surrounding areas. For example, the  
512 simulated SO<sub>2</sub>, NO<sub>2</sub> and PM<sub>2.5</sub> concentrations in Nanjing were 1.4, 1.3 and 1.2 times  
513 of those in its nearby cities. The analogous numbers for Hangzhou were 2.5, 1.5 and  
514 1.3. In contrast, the simulated O<sub>3</sub> concentrations were smaller in urban areas and  
515 larger in suburban ones. For instance, the simulated O<sub>3</sub> in Nanjing, Shanghai, Hefei  
516 and Hangzhou were 0.7, 0.4, 0.6 and 0.6 times of those in their surrounding areas,  
517 respectively. The spatial distributions of the simulated NO<sub>2</sub> and O<sub>3</sub> concentrations in  
518 Figure 2 also indicated that O<sub>3</sub> concentrations were less in the regions with higher  
519 NO<sub>2</sub> concentrations, such as the megacity of Shanghai. The simulated high  
520 concentrations of NO<sub>2</sub> in urban areas promotes titration of O<sub>3</sub>, reducing its  
521 concentrations. In addition, O<sub>3</sub> concentrations could remain relatively high after  
522 transport from urban to the suburban areas due to relatively small emissions of NO<sub>x</sub>  
523 in the latter.

### 524 3.1.2 Benefits of the “ultra-low” emission controls on air quality

525 Table 3 summarizes the absolute and relative changes of the simulated monthly  
526 concentrations of the concerned air pollutants in Cases 3-5 compared to the base case  
527 (Case 2). The average contributions of the power sector to the total ambient

528 concentrations of SO<sub>2</sub>, NO<sub>2</sub> and PM<sub>2.5</sub> for the four simulated months are estimated at  
529 10.0%, 4.7%, and 2.3%, respectively, based on comparison of Cases 2 and 5. The  
530 contributions to the concentrations were close to those of emissions at 10.7%, 6.6%,  
531 and 1.6% for the three species (as indicated in Table 1), respectively. The larger power  
532 sector contribution to the ambient PM<sub>2.5</sub> concentrations than to primary PM emissions  
533 reflects high emissions of precursors of secondary sulfate and nitrate aerosols. In  
534 general, limited contributions from the power sector were found for all concerned  
535 species except SO<sub>2</sub>, attributed to the gradually improved controls in the sector. The  
536 further implementation of the ultra-low emission policy in the sector, therefore, is  
537 expected to result in limited additional benefits for air quality. As shown in Table 3,  
538 the absolute changes of the simulated SO<sub>2</sub>, NO<sub>2</sub>, O<sub>3</sub> and PM<sub>2.5</sub> concentrations in Case  
539 3 compared to Case 2 were all smaller than 1 µg/m<sup>3</sup> for the four months. Larger  
540 changes were found for primary pollutants (SO<sub>2</sub> and NO<sub>2</sub>) than those of secondary  
541 ones (O<sub>3</sub> and PM<sub>2.5</sub>): the simulated monthly concentrations of SO<sub>2</sub> and NO<sub>2</sub> were  
542 2.7%-6.1% and 2.0%-2.9% lower, while PM<sub>2.5</sub> was only 0.1%-1.3% lower and O<sub>3</sub>  
543 0.8%-2.2% higher, respectively. Much larger benefits were found when the ultra-low  
544 emission policy was broadened from the power sector to the industrial sector (Case 4),  
545 attributed to the dominant role of industry in air pollutant emissions in the YRD  
546 region (Table 1). The simulated monthly concentrations of SO<sub>2</sub>, NO<sub>2</sub> and PM<sub>2.5</sub> were  
547 1.5-2.0, 2.5-3.7, and 4.6-6.5 µg/m<sup>3</sup> lower compared to the base case, respectively, or  
548 reduction rates of 32.9%-64.1%, 16.4%-22.8%, and 6.2%-21.6%. In contrast, the  
549 simulated O<sub>3</sub> concentration was 0.8-4.8 µg/m<sup>3</sup> higher, with growth rates ranging  
550 2.6%-14.0%. As mentioned earlier, the YRD was identified as a VOC-limited region,  
551 and reducing NO<sub>x</sub> emissions without any VOC controls would enhance O<sub>3</sub>  
552 concentrations. Currently, CEMS does not report VOCs concentration in the flue gas,  
553 and the “ultra-low emission” policy does not include VOC limit, either. In order to  
554 alleviate regional air pollution including O<sub>3</sub>, coordinated controls of NO<sub>x</sub> and VOC  
555 emissions are urgently required. These would include measures to reduce large  
556 sources of VOCs, notably in non-power industries such as chemicals and refining and  
557 in solvent use (Zhao et al., 2017).

删除的内容: S2

删除的内容: S2

删除的内容: therefore,

558 The relative changes in the simulated pollutant concentrations varied by month,  
559 due to the combined influences of meteorology and secondary chemistry, and larger  
560 relative changes were found for SO<sub>2</sub> and PM<sub>2.5</sub> in summer. As shown in Table 3, for

564 example, the average simulated PM<sub>2.5</sub> concentrations in July were 0.4 and 6.5 μg/m<sup>3</sup>  
565 lower respectively under Cases 3 and 4 compared to Case 2, with the larger reduction  
566 than other three months. This could result partly from the faster response of ambient  
567 concentrations to the changed emissions of air pollutants with shorter lifetimes in  
568 summer. The formation of secondary pollutants like PM<sub>2.5</sub> would be enhanced in  
569 summer, with more oxidative atmospheric conditions under high temperature and  
570 strong sunlight. Moreover, the relatively low concentrations in summer also  
571 contributed to the largest percentage changes in SO<sub>2</sub> and PM<sub>2.5</sub> simulation for the  
572 season.

删除的内容: Moreover, t

带格式的: 非上标/ 下标

573 Figures 3 and 4 illustrate the spatial distributions of the relative changes of  
574 simulated pollutant concentrations in Cases 3 and 4 compared to Case 2, respectively.  
575 As shown in Figure 3, the overall changes across the region due to ultra-low emission  
576 controls in the power sector only were less than 10% for primary pollutants SO<sub>2</sub> and  
577 NO<sub>2</sub>, and 5% for secondary pollutants PM<sub>2.5</sub> and O<sub>3</sub>. Larger changes in simulated SO<sub>2</sub>  
578 concentrations were found in central and northern Anhui as well as central and  
579 southern Jiangsu, with relatively concentrated distribution of coal-fired power plants.  
580 The changes of simulated SO<sub>2</sub> and NO<sub>2</sub> in Shanghai were tiny, due to few remaining  
581 power plants subject to the ultra-low emission policy and thus few emission  
582 reductions. Compared to Case 2, the SO<sub>2</sub> and NO<sub>x</sub> emissions in Case 3 were  
583 estimated to be 2.2% and 0.8% lower respectively for Shanghai, much smaller than  
584 for other provinces (6.1% and 2.5% for Anhui, 9.5% and 4.4% for Jiangsu, 5.5% and  
585 2.7% for Zhejiang). The results suggest that the potential of emission reduction and  
586 air quality improvement is limited from implementation of more stringent control  
587 measures in the power sector alone, particularly in highly developed cities where air  
588 pollution controls have already reached a relatively high level.

589 In Case 4, where both power plants and selected industrial sources meet the  
590 ultra-low emission requirement, the average reduction rates of simulated SO<sub>2</sub> and NO<sub>2</sub>  
591 concentrations compared to Case 2 were above 40% and 25% respectively for the  
592 whole region, and the changes of secondary pollutants O<sub>3</sub> and PM<sub>2.5</sub> were also  
593 significantly larger than those of Case 3 in most of the region. The relative changes of  
594 SO<sub>2</sub> were found to be more significant than other species, as the SO<sub>2</sub> concentrations  
595 are greatly affected by primary emissions. Due to the large number and wide  
596 distribution of industrial plants throughout the YRD, moreover, there was little

删除的内容: plant

删除的内容: boilers



600 regional disparity in the changed ambient SO<sub>2</sub> levels. Compared to other areas, the  
601 relatively less reduction in the simulated NO<sub>2</sub> in central YRD resulted in significant  
602 enhancement of O<sub>3</sub> concentrations (note that much more reduction in NO<sub>2</sub> resulted in  
603 similar enhancement of O<sub>3</sub> in southern Anhui for October). The comparison implies  
604 that the O<sub>3</sub> formation in central YRD was more sensitive to NO<sub>x</sub> emission abatement  
605 than other VOC-limited regions in YRD. The result suggests particularly great  
606 challenge of O<sub>3</sub> pollution control in central YRD, and more efforts on VOC emission  
607 abatement would be required for those developed areas.

### 608 **3.2 Evaluation of health benefits**

#### 609 **3.2.1 PM<sub>2.5</sub> exposures in the YRD region**

610 Figure 5 illustrates the spatial distributions of PM<sub>2.5</sub> concentrations for the base  
611 case (Case 2) and the differences of Cases 3 and 4 compared to the base case. The  
612 reduction of PM<sub>2.5</sub> concentrations from the implementation of the ultra-low emission  
613 policy in the power sector was less than 1 µg/m<sup>3</sup> over the YRD region (Figure 5b).  
614 Larger reductions (above 0.4 µg/m<sup>3</sup>) were found in northern Anhui and northern and  
615 southern Jiangsu provinces, as those regions are the energy base of eastern China,  
616 with abundant coal mines and power plants with large installed capacities. With the  
617 policy expanded to certain industrial sectors, the simulated average PM<sub>2.5</sub>  
618 concentrations were 5.8 µg/m<sup>3</sup> lower for the whole region (Figure 5c). In particular,  
619 the difference was greater than 10 µg/m<sup>3</sup> along the Yangtze River, as there are many  
620 industrial parks located along the river containing a large number of big cement, iron  
621 & steel, and chemical industry plants. Stringent emission controls at those plants  
622 would result in significant benefits in air quality for local residents.

623 We further calculated the fractions of the population with different annual  
624 average PM<sub>2.5</sub> exposure levels in Cases 2-4, as shown in Figure 6. Compared to Case  
625 2, slight differences in the population distribution by exposure level were found in  
626 Case 3, while the differences were much more significant in Case 4. The population  
627 fractions exposed to the average annual concentrations of PM<sub>2.5</sub> smaller than 35 µg/m<sup>3</sup>,  
628 35-45 µg/m<sup>3</sup> and 45-55 µg/m<sup>3</sup> were estimated to grow from 14% in Case 2 to 21% in  
629 Case 4, from 11% to 16%, and from 16% to 30%, respectively. (note 35 µg/m<sup>3</sup> is the  
630 annual PM<sub>2.5</sub> concentration limit in the current National Ambient Air Quality Standard

删除的内容: In the central YRD, including Shanghai, northern Zhejiang and southern Jiangsu, the changes in simulated NO<sub>2</sub> were modest, resulting in clear enhancement of O<sub>3</sub> concentrations. The result suggests the great challenges of O<sub>3</sub> pollution abatement in those developed areas, even with aggressive measures on NO<sub>x</sub> control at power and industrial plants. .

删除的内容: boiler

删除的内容: s

带格式的: 非上标/ 下标

带格式的: 非上标/ 下标

带格式的: 下标

带格式的: 非上标/ 下标

带格式的: 非上标/ 下标

带格式的: 非上标/ 下标

644 | for China). Accordingly, the fraction exposed to PM<sub>2.5</sub> concentrations larger than 55  
645 | µg/m<sup>3</sup> declined from 59% to 33%. The implementation of ultra-low emission policy  
646 | on both power plants and industry sources thus proved an effective way in limiting the  
647 | population exposed to high PM<sub>2.5</sub> levels.

删除的内容: secto

删除的内容: r

删除的内容: s

### 648 | 3.2.2 Human health risk with base case emissions

649 | The mortality and YLL caused by atmospheric PM<sub>2.5</sub> exposure with the base case  
650 | emissions (Case 2) in the YRD region are shown in Table 4. The values in brackets  
651 | represent the 95% confidence interval (CI) attributed to the uncertainty of IER curves  
652 | (i.e., uncertainties from other sources were excluded in the 95% CI estimation such as  
653 | air quality model mechanisms, emission inventories, and population data). With the  
654 | base case emissions, the NMB of the simulated and observed annual PM<sub>2.5</sub>  
655 | concentrations (based on the four representative months) was calculated at -1.4% for  
656 | the YRD region. Therefore, the influence of the biases between the simulations and  
657 | observations on the estimated health risks was negligible and thus not considered in  
658 | this study. The total attributable deaths due to all diseases caused by PM<sub>2.5</sub> exposure in  
659 | the YRD region were estimated at 194,000 (114,000-282,000), with STK, IHD and  
660 | COPD causing the most deaths, accounting for 29%, 32% and 22% of the total  
661 | respectively. With larger populations in Anhui and Jiangsu (32% and 37% of the  
662 | regional total respectively), more deaths caused by PM<sub>2.5</sub> exposure were found in  
663 | these two provinces, at 34% and 41% of the total deaths respectively. Among all the  
664 | diseases, STK was found to cause the largest number of mortalities (19,600) in Anhui  
665 | with PM<sub>2.5</sub> exposure, IHD in Jiangsu (31,300), and COPD in Shanghai (4,400) and  
666 | Zhejiang (10,800). The total YLL caused by PM<sub>2.5</sub> exposure in the YRD region was  
667 | 5.11 million years (3.16 - 7.18 million years). More YLL caused by PM<sub>2.5</sub> exposure  
668 | was found in Anhui and Jiangsu, accounting for 34% and 37% of the total in the YRD  
669 | region respectively. YLL caused by COPD were the largest in all the provinces, with  
670 | 0.66, 0.19, 0.56 and 0.47 million years estimated for Anhui, Shanghai, Jiangsu and  
671 | Zhejiang, respectively. The spatial distribution of attributable deaths and YLL caused  
672 | by PM<sub>2.5</sub> exposure was basically consistent with that of population in the YRD region,  
673 | with correlation coefficients of 0.94 and 0.96 respectively. As shown in Figure 7,  
674 | higher health risks attributed to PM<sub>2.5</sub> pollution in the base case (Case 2) were  
675 | commonly found in the areas with larger population densities, including the areas

删除的内容: under

删除的内容: , all with higher population densities

680 | along the Yangtze River, central Shanghai and some urban areas in Anhui. We further  
681 | compared the population deaths attributable to PM<sub>2.5</sub> exposure calculated in this study  
682 | with the reported total deaths in provincial statistical yearbooks (AHBS, 2016; JSBS,  
683 | 2016; SHBS, 2016; ZJBS, 2016), and found that the deaths caused by PM<sub>2.5</sub> exposure  
684 | accounted for 18%, 14%, 15% and 11% of the total deaths in Anhui, Jiangsu,  
685 | Shanghai and Zhejiang respectively for 2015. The numbers were larger than the  
686 | estimate (6.9%) by Maji et al. (2018), which focused on 161 cities in China. As one of  
687 | the most developed and industrialized regions in China, YRD suffered higher PM<sub>2.5</sub>  
688 | pollution level than the national average, leading to the larger fraction of premature  
689 | death due to PM<sub>2.5</sub> exposure. Moreover, the baseline disease-specific mortality rates  
690 | applied in this study (from GHDx) were commonly higher than those in Maji et al.  
691 | (2018) except for LRI, resulting in the larger estimate of death rates exposed to PM<sub>2.5</sub>.

692 | Many studies have focused on the human health risks attributable to air pollution  
693 | in China, with considerable disparities between them due to different estimation  
694 | methods and health endpoints selected. Figure 8 compares the estimates of premature  
695 | deaths caused by PM<sub>2.5</sub> exposure in the YRD region in this and previous studies.  
696 | Relatively close results are found between studies for the same regions and periods.  
697 | For example, Hu et al. (2017) and Liu et al. (2016) estimated that the premature  
698 | deaths of adults (>30 years old) due to PM<sub>2.5</sub> exposure were 223,000 and 245,000  
699 | respectively in 2013 in the YRD region. However, the health endpoints in these two  
700 | studies were not completely consistent. COPD, LC, IHD and CEV (cerebrovascular  
701 | disease) were selected in Hu et al. (2017), while COPD, LC, IHD and STK were  
702 | chosen by Liu et al. (2016). The deaths caused by PM<sub>2.5</sub> exposure in Shanghai were  
703 | estimated at 19,000, 15,000, and 16,000 respectively in Maji et al. (2018), Song et al.  
704 | (2017) and this study, respectively. The IER model and the same health endpoints  
705 | were adopted in all three studies, while the PM<sub>2.5</sub> concentrations were derived from  
706 | ground observations in the former two studies instead of air quality simulation in this  
707 | study. The premature deaths attributable to PM<sub>2.5</sub> exposure in the YRD region in 2015  
708 | were estimated at 122,000 in Maji et al. (2018) and 194,000 in this study respectively.

709 | Besides the different baseline mortality rates adopted in the two studies as mentioned  
710 | earlier, the smaller estimate by Maji et al. (2018) could also result partly from  
711 | inclusion of only typical cities instead of all cities in the YRD region. There are clear  
712 | disparities in estimates of premature deaths for different years. For example, the death

删除的内容: , with

删除的内容: discrepancy

删除的内容: ing

删除的内容: in part

删除的内容: of

删除的内容: in the estimation of the former

722 estimates caused by PM<sub>2.5</sub> exposure in 2015 were generally smaller than those in 2013.  
723 As the population and age distributions remained relatively stable over the two years  
724 (AHBS, 2016; JSBS, 2016; SHBS, 2016; ZJBS, 2016), the reduced estimated  
725 premature deaths result to some extent from emission abatement and air quality  
726 improvement. According to relevant studies of Shanghai in particular (Lelieveld et al.,  
727 2013; 2015; Liu et al., 2016; Xie et al., 2016; Hu et al., 2017; Song et al., 2017; Maji  
728 et al., 2018), the premature deaths attributable to PM<sub>2.5</sub> exposure increased from 2005  
729 to 2013 and then declined afterwards, reflecting the health benefit of air pollution  
730 control measures in Shanghai in recent years.

### 731 3.2.3 Benefits of emission controls on human health

732 Tables 5 and 6 respectively summarize the avoided premature deaths and YLL by  
733 disease and region that would result from implementation of the ultra-low emission  
734 control policy and thereby reduced PM<sub>2.5</sub> pollution in the YRD region. If only the  
735 coal-fired power sector meet the ultra-low emission limits (Case 3), nearly 305  
736 premature deaths would be avoided compared to the base case emissions in 2015,  
737 with a tiny reduction rate of only 0.16%. If the policy is strictly implemented for  
738 selected industrial sectors as well (Case 4), 10,651 premature deaths could be avoided  
739 with a reduction rate at 5.50%. The largest numbers of avoided premature deaths were  
740 found in Anhui and Jiangsu, accounting collectively for 88.2% and 68.7% of the total  
741 avoided deaths in Cases 3 and 4 respectively. The greatest impacts from reduced  
742 PM<sub>2.5</sub> concentrations were found for STK, of which the avoided deaths were  
743 calculated at 85 and 2848 in Cases 3 and 4, respectively. The health effects of  
744 emission control policies in the YRD region have been investigated in previous  
745 studies. Using the IER model, Dai et al. (2019) chose the premature deaths from IHD,  
746 CEV, COPD and LC as health endpoints, and found that the Clean Air Action Plan  
747 would avoid 3,439 deaths caused by PM<sub>2.5</sub> exposure in Shanghai, more than those in  
748 both Case 3 and Case 4 in this study (5 and 1,185 respectively). Applying  
749 environmental health risk and valuation methods, Li and Li (2018) found that 15,709  
750 premature deaths attributable to air pollution could be avoided in 2015 if the PM<sub>2.5</sub>  
751 concentrations in Jiangsu province were assumed to meet the National Ambient Air  
752 Quality Standard (GB3095-2012, 35 µg/m<sup>3</sup> as the annual average). The estimate is  
753 much more than those calculated in Case 3 and Case 4 (177 and 4,114 deaths

删除的内容: the

755 respectively). The larger health benefits estimated in those two studies result from  
756 their assumption of emission control measures covering a much wider range of sectors  
757 including energy, industry, transportation, construction, and agriculture, while only the  
758 ultra-low emission policy was assumed for the power and industry sectors in this  
759 study. The comparisons illustrate that the health benefits from emission control in the  
760 power sector alone is limited, and that controls in other sectors are essential. In  
761 addition, the different methods and inconsistent data sources partly led to the  
762 discrepancies. For the particle exposure estimation, as an example, Dai et al. (2019)  
763 adopted the BENMAP-CE model (Environmental Benefits Mapping and Analysis  
764 Program-Community Edition, Yang et al. (2013)) to simulate the ambient PM<sub>2.5</sub>  
765 concentrations, while Li and Li (2018) used the average of monitored PM<sub>2.5</sub>  
766 concentrations. As shown in Table 6, the avoided YLL for Case 3 and Case 4 were  
767 estimated at 8744 and 316,562 years respectively compared to the base case,  
768 confirming again the greatly improved health benefits from implementation of  
769 ultra-low emission policy for the industry sector in addition to the power sector. The  
770 largest avoided YLL were found in Anhui and Jiangsu in the YRD region, accounting  
771 collectively for 86% and 65% of the total avoided YLL in Cases 3 and 4 respectively.  
772 Compared to Case 3, the fractions of Shanghai and Zhejiang to total YRD for both  
773 avoided deaths (Table 5) and YLL (Table 6) were clearly higher in Case 4, implying a  
774 greater health benefit of emission controls at industry sources in these relatively  
775 industrialized urban regions. The reduced PM<sub>2.5</sub> concentrations led to the largest  
776 avoided YLL of COPD in both cases (3,118 and 119,300 years in Cases 3 and 4,  
777 respectively).

778 Figure 9 illustrates the spatial distributions of the avoided deaths and YLL from  
779 the ultra-low emission policy in the YRD region. When the policy was implemented  
780 only for coal-fired power plants, the health benefits were small and the regional  
781 differences relatively insignificant, with the avoided deaths and YLL smaller than 10  
782 persons and 100 years respectively for all of the grid cells (Figure 9a and 9b). When  
783 the policy was implemented both in power and industry sectors, more avoided deaths  
784 (>40 person/grid cell) and YLL (>400 years/grid cell) were found in northern Anhui,  
785 southern Jiangsu, central Shanghai and northern Zhejiang (Figure 9c and 9d). The  
786 spatial correlation coefficient between the avoided YLL in Case 4 and population was  
787 0.93, indicating that the implementation of the emission control policy would lead to

删除的内容: Comparing

删除的内容: to Case 4,

删除的内容: for Shanghai and part of  
Zhejiang

792 greater health benefits for areas with intensive economic activity and dense  
793 populations.

794

#### 795 **4. Conclusions**

796 We evaluated the improvement of emission estimation by incorporating CEMS  
797 data for the power sector, and explored the air quality and health benefits from the  
798 ultra-low emission control policy for the YRD region through air quality modeling. In  
799 general, the bias between ground observations and simulations based on the emission  
800 inventory with CEMS data incorporated was smaller than that without, suggesting that  
801 appropriate use of online monitoring information helped improve the emission  
802 estimation and model performance. Compared to the base case in which CEMS data  
803 were incorporated in emission estimation, the simulated monthly concentrations of all  
804 the concerned species (SO<sub>2</sub>, NO<sub>2</sub>, O<sub>3</sub>, and PM<sub>2.5</sub>) differed less than 7% when the  
805 ultra-low emission policy was enacted only in the coal-fired power sector, given its  
806 small fraction of total emissions. When the policy was implemented for selected  
807 industrial sectors as well, larger differences in air quality from the base case were  
808 found, with the simulated concentrations of SO<sub>2</sub>, NO<sub>2</sub> and PM<sub>2.5</sub> respectively  
809 33%-64%, 16%-23% and 6%-22% lower and O<sub>3</sub> 3%-14% higher, depending on the  
810 month.

删除的内容: the

811 Nearly 305 premature deaths and 8,744 years of YLL would be avoided if the  
812 policy was implemented for the power sector alone, and benefits would reach 10,651  
813 premature deaths and 316,562 YLL avoided with the policy enacted for both power  
814 and industrial sectors. The study revealed the limited potential for further emission  
815 reduction and air quality improvement via controls in the power sector alone. Along  
816 with stringent emission control in that sector, the coordinated control of emissions  
817 from non-power industrial sources would be essential to effectively improve air  
818 quality and reduce associated human health risks. Moreover, more attention needs to  
819 be paid to control of VOC to limit O<sub>3</sub> formation resulting from reduction of NO<sub>x</sub> in  
820 the region.

删除的内容: y

821

## 824 **Data availability**

825 All data in this study are available from the authors upon request.

## 826 **Author contributions**

827 YZhang developed the strategy and methodology of the work and wrote the draft.  
828 YZhao improved the methodology and revised the manuscript. MG provided useful  
829 comments on the health risk analysis. XB provided emission monitoring data. CPN  
830 revised the manuscript.

## 831 **Competing interests**

832 The authors declare that they have no conflict of interest.

## 833 **Acknowledgments**

834 This work was sponsored by the Natural Science Foundation of China (41922052 and  
835 91644220), National Key Research and Development Program of China  
836 (2017YFC0210106), and a Harvard Global Institute award to the Harvard-China  
837 Project on Energy, Economy and Environment. We would also like to thank Tsinghua  
838 University for the free use of national emissions data (MEIC).

## 839 **References**

- 840 An, X., Sun, Z., Lin, W., Jin, M., and Li, N.: Emission inventory evaluation using  
841 observations of regional atmospheric background stations of China, *J. Environ.*  
842 *Sci.*, 25, 537-536, 2013.
- 843 AHBS (Anhui Bureau of Statistics): *Statistical Yearbook of Anhui*, China Statistics  
844 Press, Beijing, 2016 (in Chinese).
- 845 Baker, K., Johnson, M., and King, S.: Meteorological modeling performance  
846 summary for application to PM<sub>2.5</sub>/haze/ozone modeling projects, Lake Michigan  
847 Air Directors Consortium, Midwest Regional Planning Organization, Des Plaines,  
848 Illinois, USA, 57 pp, 2004.
- 849 Butt, E. W., Turnock, S. T., Rigby, R., Reddington, C. L., Yoshioka, M., Johnson, J. S.,  
850 Regayre, L. A., Pringle, K. J., Mann, G. W., and Spracklen, D. V.: Global and

851 regional trends in particulate air pollution and attributable health burden over the  
852 past 50 years, *Environ. Res. Lett.*, 12, 10.1088/1748-9326/aa87be, 2017.

853 Chang, X., Wang, S., Zhao, B., Xing, J., Liu, X., Wei, L., Song, Y., Wu, W., Cai, S.,  
854 Zheng, H., Ding, D., and Zheng, M.: Contributions of inter-city and regional  
855 transport to PM<sub>2.5</sub> concentrations in the Beijing-Tianjin-Hebei region and its  
856 implications on regional joint air pollution control, *Sci. Total. Environ.*, 660,  
857 1191-1200, 10.1016/j.scitotenv.2018.12.474, 2019.

858 Cohen, A. J., Brauer, M., Burnett, R., Anderson, H. R., Frostad, J., Estep, K., et al.:  
859 Estimates and 25-year trends of the global burden of disease attributable to  
860 ambient air pollution: an analysis of data from the Global Burden of Diseases  
861 Study 2015, *Lancet*, 389, 1907-1918, 2017.

862 Dai, H. X., An, J. Y., Li, L., Huang, C., Yan, R. S., Zhu, S. H., Ma, Y. G., Song, W. M.,  
863 and Kan, H. D.: Health Benefit Analyses of the Clean Air Action Plan  
864 Implementation in Shanghai, *Environmental Science*, 40, 1, 10.13227  
865 /j.hjcx.201804201, 2019 (in Chinese).

866 Dockery, D. W., Pope, C. A., Xu, X. P., Spengler, J. D., Ware, J. H., Fay, M. E., Ferris,  
867 B. G., and Speizer, F. E.: An Association between air-pollution and mortality in 6  
868 United-States cities, *N. Engl. J. Med.*, 329, 1753-1759,  
869 10.1056/nejm199312093292401, 1993.

870 Emery, C., Tai, E., and Yarwood, G.: Enhanced meteorological modeling and  
871 performance evaluation for two Texas episodes, Report to the Texas Natural  
872 Resources Conservation Commission, prepared by ENVIRON, International  
873 Corp, Novato, CA, 2001.

874 Fu, J. S., Jang, C. J., Streets, D. G., Li, Z., Kwok, R., Park, R., and Han, Z.:  
875 MICS-Asia II: Modeling gaseous pollutants and evaluating an advanced  
876 modeling system over East Asia, *Atmos. Environ.*, 42, 3571-3583,  
877 10.1016/j.atmosenv.2007.07.058, 2008.

878 Gao, J., Wang, T., Ding, A. J., and Liu, C. B.: Observational study of ozone and  
879 carbon monoxide at the summit of mount Tai (1534 m a.s.l.) in central-eastern  
880 China, *Atmos. Environ.*, 39, 4779-4791, 10.1016/j.atmosenv.2005.04.030, 2005.

881 Gao, J. H., Zhu, B., Xiao, H., Kang, H. Q., Hou, X. W., and Shao, P.: A case study of  
882 surface ozone source apportionment during a high concentration episode, under  
883 frequent shifting wind conditions over the Yangtze River Delta, China, *Sci. Total*



884 Environ., 544, 853-863, 2016.

885 Gao, M., Beig, G., Song, S., Zhang, H., Hu, J., Ying, Q., Liang, F., Liu, Y., Wang, H.,  
886 Lu, X., Zhu, T., Carmichael, G. R., Nielsen, C. P., and McElroy, M. B.: The  
887 impact of power generation emissions on ambient PM<sub>2.5</sub> pollution and human  
888 health in China and India, *Environ. Int.*, 121, 250-259,  
889 10.1016/j.envint.2018.09.015, 2018.

890 Gleser, L. J.: Bootstrap confidence intervals, *Statistical Science*, 11, 219-221, 1996.

891 Guenther, A. B., Jiang, X., Heald, C. L., Sakulyanontvittaya, T., Duhl, T., Emmons, L.  
892 K., and Wang, X.: The Model of Emissions of Gases and Aerosols from Nature  
893 version 2.1 (MEGAN2.1): an extended and updated framework for modeling  
894 biogenic emissions, *Geosci. Model Dev.*, 5, 1471-1492, 2012.

895 Han, K. M., Lee, S., Chang, L. S., and Song, C. H.: A comparison study between  
896 CMAQ-simulated and OMI-retrieved NO<sub>2</sub> columns over East Asia for evaluation  
897 of NO<sub>x</sub> emission fluxes of INTEX-B, CAPSS, and REAS inventories, *Atmos.*  
898 *Chem. Phys.*, 15, 1913-1938, 10.5194/acp-15-1913-2015, 2015.

899 He, J. J., Yu, Y., Yu, L. J., Liu, N., and Zhao, S. P.: Impacts of uncertainty in land  
900 surface information on simulated surface temperature and precipitation over  
901 China, *Int. J. Climatol.*, 10.1002/joc.5041, 2017.

902 Hoek, G., Krishnan, R. M., Beelen, R., Peters, A., Ostro, B., Brunekreef, B., and  
903 Kaufman, J. D.: Long-term air pollution exposure and cardio- respiratory  
904 mortality: a review, *Environmental Health*, 12, 10.1186/1476-069x-12-43, 2013.

905 Hu, J., Huang, L., Chen, M., Liao, H., and Ying, Q.: Premature mortality attributable  
906 to particulate matter in China: source contributions and responses to reductions,  
907 *Environ. Sci. Technol.*, 51, 9950-9959, 2017.

908 Huang, C., Chen, C. H., Li, L., Cheng, Z., Wang, H. L., Huang, H. Y., Streets, D. G.,  
909 Wang, Y. J., Zhang, G. F., and Chen, Y. R.: Emission inventory of anthropogenic  
910 air pollutants and VOC species in the Yangtze River Delta region, China, *Atmos.*  
911 *Chem. Phys.*, 11, 4105-4120, 10.5194/acp-11-4105-2011, 2011.

912 JSBS (Jiangsu Bureau of Statistics): *Statistical Yearbook of Jiangsu*, China Statistics  
913 Press, Beijing, 2016 (in Chinese).

914 Lei, Y., Xue, W. B., Zhang, Y. S., and Xu, Y. L.: Health benefit evaluation for air  
915 pollution prevention and control action plan in China, *Chinese Environmental*  
916 *Management*, 5, 10.16868/j.cnki.1674-6252.2015.05.009, 2015 (in Chinese).

- 917 Lelieveld, J., Barlas, C., Giannadaki, D., and Pozzer, A.: Model calculated global,  
918 regional and megacity premature mortality due to air pollution, *Atmos. Chem.*  
919 *Phys.*, 13, 7023-7037, 10.5194/acp-13-7023-2013, 2013.
- 920 Lelieveld, J., Evans, J. S., Fnais, M., Giannadaki, D., and Pozzer, A.: The contribution  
921 of outdoor air pollution sources to premature mortality on a global scale, *Nature*,  
922 525, 367-371, 10.1038/nature15371, 2015.
- 923 Li, H. J., and Li, M. Q.: Assessment on health benefit of air pollution control in  
924 Jiangsu province, *Chinese Public Health*, 34, 12, 10.11847/zgggws1117789,  
925 2018 (in Chinese).
- 926 Li, L., Chen, C. H., Fu, J. S., Huang, C., Streets, D. G., Huang, H. Y., Zhang, G. F.,  
927 Wang, Y. J., Jang, C. J., Wang, H. L., Chen, Y. R., and Fu, J. M.: Air quality and  
928 emissions in the Yangtze River Delta, China, *Atmos. Chem. Phys.*, 11,  
929 1621-1639, 10.5194/acp-11-1621-2011, 2011.
- 930 Li, L., Chen, C. H., Huang, C., Huang, H. Y., Zhang, G. F., Wang, Y. J., Wang, H. L.,  
931 Lou, S. R., Qiao, L. P., Zhou, M., Chen, M. H., Chen, Y. R., Streets, D. G., Fu, J.  
932 S., and Jang, C. J.: Process analysis of regional ozone formation over the Yangtze  
933 River Delta, China using the Community Multi-scale Air Quality modeling  
934 system, *Atmos. Chem. Phys.*, 12, 10971-10987, 10.5194/acp-12-10971-2012,  
935 2012.
- 936 Li, L., An, J. Y., and Lu, Q.: Modeling Assessment of PM<sub>2.5</sub> Concentrations Under  
937 implementation of Clean Air Action Plan in the Yangtze River Delta Region,  
938 *Research of Environmental Sciences*, 28, 1653-1661,  
939 10.13198/j.issn.1001-6929.2015.11.01, 2015 (in Chinese).
- 940 Li, M., Zhang, D., Li, C.-T., Selin, N.E., and Karplus, V.J.: Co-benefits of China's  
941 climate policy for air quality and human health in China and transboundary  
942 regions in 2030, *Environ. Res. Lett.*, 14, 10.1038/s41558-018-0139-4, 2019.
- 943 Liao, J. B., Wang, T. J., Jiang, Z.Q., Zhuang, B. L., Xie, M., Yin, C. Q., Wang, X. M.,  
944 Zhu, J. L., Fu, Y., and Zhang, Y.: WRF/Chem modeling of the impacts of urban  
945 expansion on regional climate and air pollutants in Yangtze River Delta, China,  
946 *Atmos. Environ.*, 106, 204-214, 10.1016/j.atmosenv.2015.01.059, 2015.
- 947 Lim, S. S., Vos, T., Flaxman, A. D., Danaei, G., Shibuya, K., Adair-Rohani, H., et al.:  
948 A comparative risk assessment of burden of disease and injury attributable to 67  
949 risk factors and risk factor clusters in 21 regions, 1990-2010: a systematic

删除的内容: .

951 analysis for the Global Burden of Disease Study 2010, *Lancet*, 380, 2224-2260,  
952 2012.

953 Liu, J., Han, Y., Tang, X., Zhu, J., and Zhu, T.: Estimating adult mortality attributable  
954 to PM<sub>2.5</sub> exposure in China with assimilated PM<sub>2.5</sub> concentrations based on a  
955 ground monitoring network, *Sci. Total Environ.*, 568, 1253-1262, 2016.

956 Liu, X., Gao, X., Wu, X., Yu, W., Chen, L., Ni, R., Zhao, Y., Duan, H., Zhao, F., Chen,  
957 L., Gao, S., Xu, K., Lin, J., and Ku, A. Y.: Updated Hourly Emissions Factors for  
958 Chinese Power Plants Showing the Impact of Widespread Ultralow Emissions  
959 Technology Deployment, *Environ. Sci. Technol.*, 53, 2570-2578,  
960 10.1021/acs.est.8b07241, 2019.

961 Liu, X. H., Zhang, Y., Xing, J., Zhang, Q., Wang, K., Streets, D. G., Jiang, C., Wang,  
962 W. X., and Hao, J. M.: Understanding of regional air pollution over China using  
963 CMAQ, part II. Process analysis and sensitivity of ozone and particulate matter  
964 to precursor emissions, *Atmos. Environ.*, 44, 3719-3727,  
965 10.1016/j.atmosenv.2010.03.036, 2010.

966 Lu, Y., Zhao, X., Zhao, Y.: The comparison and evaluation of air pollutant simulation  
967 for the Yangtze River Delta region with different versions of air quality model.  
968 *Environ. Monit. Forewarn.* 12, 10.3969/j.issn.1674-6732.2020.03.001, 2020 (in  
969 Chinese).

970 Maji, K. J., Dikshit, A. K., Arora, M., and Deshpande, A.: Estimating premature  
971 mortality attributable to PM<sub>2.5</sub> exposure and benefit of air pollution control  
972 policies in China for 2020, *Sci. Total Environ.*, 612, 683-693,  
973 10.1016/j.scitotenv.2017.08.254, 2018.

974 Ohara, T., Akimoto, H., Kurokawa, J., Horii, N., Yamaji, K., Yan, X., and Hayasaka,  
975 T.: An Asian emission inventory of anthropogenic emission sources for the  
976 period 1980-2020, *Atmos. Chem. Phys.*, 7, 4419-4444, 2007.

977 Price, C., Penner, J., and Prather, M.: NO<sub>x</sub> from lightning: 1. Global distribution  
978 based on lightning physics, *J. Geophys. Res.-Atmos.*, 102, 5929-5941,  
979 10.1029/96jd03504, 1997.

980 Shanghai Bureau of Statistics (SHBS): Statistical Yearbook of Shanghai, China  
981 Statistics Press, Beijing, 2016 (in Chinese).

982 Sindelarova, K., Granier, C., Bouarar, I., Guenther, A., Tilmes, S., Stavrakou, T.,  
983 Muller, J. F., Kuhn, U., Stefani, P., and Knorr, W.: Global data set of biogenic

刪除的內容: .

985 VOC emissions calculated by the MEGAN model over the last 30 years, *Atmos.*  
986 *Chem. Phys.*, 14, 9317-9341, 10.5194/acp-14-9317-2014, 2014.

987 Skamarock, W. C., Klemp, J. B., Dudhia, J., Gill, D. O., Barker, D. M., Duda, M. G.,  
988 Huang, X.-Y., Wang, W., and Powers, J. G.: A Description of the Advanced  
989 Research WRF Version 3, NCAR Tech. Note NCAR/TN-475+STR, 113 pp.,  
990 10.5065/D68S4MVH, 2008.

991 Song, C., He, J., Wu, L., Jin, T., Chen, X., Li, R., Ren, P., Zhang, L., and Mao, H.:  
992 Health burden attributable to ambient PM<sub>2.5</sub> in China, *Environ. Pollut.*, 223,  
993 575-586, 2017.

994 Tan, J., Fu, J. S., Huang, K., Yang, C.-E., Zhuang, G., and Sun, J.: Effectiveness of  
995 SO<sub>2</sub> emission control policy on power plants in the Yangtze River Delta,  
996 China-post-assessment of the 11th Five-Year Plan, *Environ. Sci. Pollut. R.*, 24,  
997 8243-8255, 10.1007/s11356-017-8412-z, 2017.

998 Tang, L., Qu, J. B., Mi, Z. F., Bo, X., Chang, X. Y., Anadon, L. D., Wang, S. Y., Xue,  
999 X. D., Li, S. B., Wang, X., and Zhao, X. H.: Substantial emission reductions  
1000 from Chinese power plants after the introduction of ultra-low emissions  
1001 standards, *Nat. Energy*, 4, 929–938, 10.1038/s41560-019-0468-1, 2019.

1002 Tang, Y., An, J., Wang, F., Li, Y., Qu, Y., Chen, Y., and Lin, J.: Impacts of an unknown  
1003 daytime HONO source on the mixing ratio and budget of HONO, and hydroxyl,  
1004 hydroperoxyl, and organic peroxy radicals, in the coastal regions of China,  
1005 *Atmos. Chem. Phys.*, 15, 9381-9398, 10.5194/acp-15-9381-2015, 2015.

1006 University of North Carolina at Chapel Hill (UNC): Operational Guidance for the  
1007 Community Multiscale Air Quality (CMAQ) Modeling System Version 4.7.1  
1008 (June 2010 Release), available at <http://www.cmaq-model.org> (last access: 10  
1009 Feb 2020), 2010.

1010 Uno, I., He, Y., Ohara, T., Yamaji, K., Kurokawa, J. I., Katayama, M., Wang, Z.,  
1011 Noguchi, K., Hayashida, S., Richter, A., and Burrows, J. P.: Systematic analysis  
1012 of interannual and seasonal variations of model-simulated tropospheric NO<sub>2</sub> in  
1013 Asia and comparison with GOME-satellite data, *Atmos. Chem. Phys.*, 7,  
1014 1671-1681, 10.5194/acp-7-1671-2007, 2007.

1015 Wang, G., Zhang, R., Gomez, M. E., Yang, L., Levy Zamora, M., Hu, M., et al.:  
1016 Persistent sulfate formation from London Fog to Chinese haze. *P. Natl. Acad.*

- 1017 Sci., 48, 13630-13635, 10.1073/pnas.1616540113, 2016.
- 1018 Wang, K., Zhang, Y., Jang, C., Phillips, S., and Wang, B.: Modeling intercontinental  
1019 air pollution transport over the trans-Pacific region in 2001 using the Community  
1020 Multiscale Air Quality modeling system, *J. Geophys. Res.-Atmos.*, 114,  
1021 10.1029/2008jd010807, 2009.
- 1022 Wang, L. T., Jang, C., Zhang, Y., Wang, K., Zhang, Q., Streets, D. G., Fu, J., Lei, Y.,  
1023 Schreifels, J., He, K. B., Hao, J. M., Lam, Y., Lin, J., Meskhidze, N., Voorhees, S.,  
1024 Evarts, D., and Phillips, S.: Assessment of air quality benefits from national air  
1025 pollution control policies in China. Part II: Evaluation of air quality predictions  
1026 and air quality benefits assessment, *Atmos. Environ.*, 44, 3449-3457,  
1027 10.1016/j.atmosenv.2010.05.051, 2010.
- 1028 Wang, L. T., Wei, Z., Yang, J., Zhang, Y., Zhang, F. F., Su, J., Meng, C. C., and Zhang,  
1029 Q.: The 2013 severe haze over southern Hebei, China: model evaluation, source  
1030 apportionment, and policy implications, *Atmos. Chem. Phys.*, 14, 3151-3173,  
1031 10.5194/acp-14-3151-2014, 2014.
- 1032 Wang, N., Lyu, X., Deng, X., Huang, X., Jiang, F., and Ding, A.: Aggravating O<sub>3</sub>  
1033 pollution due to NO<sub>x</sub> emission control in eastern China, *Sci. Total Environ.*, 677,  
1034 732-744, 2019.
- 1035 Wang, Z., Pan, L., Li, Y., Zhang, D., Ma, J., Sun, F., Xu, W., and Wang, X.:  
1036 Assessment of air quality benefits from the national pollution control policy of  
1037 thermal power plants in China: A numerical simulation, *Atmos. Environ.*, 106,  
1038 288-304, 10.1016/j.atmosenv.2015.01.022, 2015.
- 1039 Xia, Y., Zhao, Y., and Nielsen, C. P.: Benefits of of China's efforts in gaseous pollutant  
1040 control indicated by the bottom-up emissions and satellite observations  
1041 2000-2014, *Atmos. Environ.*, 136, 43-53, 10.1016/j.atmosenv.2016.04.013, 2016.
- 1042 Xie, R., Sabel, C. E., Lu, X., Zhu, W., Kan, H., Nielsen, C. P., and Wang, H.:  
1043 Long-term trend and spatial pattern of PM<sub>2.5</sub> induced premature mortality in  
1044 China, *Environ. Int.*, 97, 180-186, 10.1016/j.envint.2016.09.003, 2016.
- 1045 Xing, J., Wang, S. X., Jang, C., Zhu, Y., and Hao, J. M.: Nonlinear response of ozone  
1046 to precursor emission changes in China: a modeling study using response surface  
1047 methodology, *Atmos. Chem. Phys.*, 11, 5027-5044, 10.5194/acp-11-5027-2011,  
1048 2011.
- 1049 Yang, C. F. O., Lin, N. H., Sheu, G. R., Lee, C. T., and Wang, J. L.: Seasonal and

带格式的: 不检查拼写或语法, 下标

1050 diurnal variations of ozone at a high-altitude mountain baseline station in East  
1051 Asia, *Atmos. Environ.*, 46, 279-288, 10.1016/j.atmosenv.2011.09.060, 2012.

1052 Yang, J., Zhao, Y., Cao, J., and Nielsen, C.: Co-benefits of carbon and pollution  
1053 control policies on air quality and health till 2030 in China, *Environ. Int.*, 152,  
1054 106482, 10.1016/j.envint.2021.106482, 2021.

1055 Yang, Y., Zhao, Y., Zhang, L., Zhang, J., Huang, X., Zhao X., Zhang, Y., Xi, M., Lu,  
1056 Y.: Improvement of the satellite-derived NO<sub>x</sub> emissions on air quality modeling  
1057 and its effect on ozone and secondary inorganic aerosol formation in the Yangtze  
1058 River Delta, China. *Atmos. Chem. Phys.*, 21, 1191-1209,  
1059 10.5194/acp-21-1191-2021, 2021

1060 Yang, Y., Zhu, Y., Jang, C., Xie, J. P., Wang, S. X., Fu, J., Lin, C. J., Ma, J., Ding, D.,  
1061 Qiu, X. Z., and Lao, Y. W.: Research and development of environmental benefits  
1062 mapping and analysis program: Community edition, *Acta Scientiae*  
1063 *Circumstantiae*, 33, 2395-2401, 10.13671/j.hjkxxb.2013.09.022, 2013 (in  
1064 Chinese).

1065 Yue, H., He, C., Huang, Q., Yin, D., and Bryan, B. A.: Stronger policy required to  
1066 substantially reduce deaths from PM<sub>2.5</sub> pollution in China, *Nat. Commun.*, 11,  
1067 1462, 10.1038/s41467-020-15319-4, 2020.

1068 Yu, S., Mathur, R., Kang, D., Schere, K., Eder, B., and Pleirn, J.: Performance and  
1069 diagnostic evaluation of ozone predictions by the eta-community multiscale air  
1070 quality forecast system during the 2002 New England Air Quality Study, *J. Air*  
1071 *Waste Manage.*, 56, 1459-1471, 10.1080/10473289.2006.10464554, 2006.

1072 Zhang, L., Zhao, T., Gong, S., Kong, S., Tang, L., Liu, D., Wang, Y., Jin, L., Shan, Y.,  
1073 Tan, C., Zhang, Y., and Guo, X.: Updated emission inventories of power plants in  
1074 simulating air quality during haze periods over East China, *Atmos. Chem. Phys.*,  
1075 18, 2065-2079, 10.5194/acp-18-2065-2018, 2018.

1076 Zhang, M., Uno, I., Zhang, R., Han, Z., Wang, Z., and Pu, Y.: Evaluation of the  
1077 Models-3 Community Multi-scale Air Quality (CMAQ) modeling system with  
1078 observations obtained during the TRACE-P experiment: Comparison of ozone  
1079 and its related species, *Atmos. Environ.*, 40, 4874-4882,  
1080 10.1016/j.atmosenv.2005.06.063, 2006.

1081 Zhang, Q., Streets, D. G., Carmichael, G. R., He, K. B., Huo, H., Kannari, A.,  
1082 Klimont, Z., Park, I. S., Reddy, S., Fu, J. S., Chen, D., Duan, L., Lei, Y., Wang, L.

带格式的: 行距: 1.5 倍行距

删除的内容: .

删除的内容: .

1085 T., and Yao, Z. L.: Asian emissions in 2006 for the NASA INTEX-B mission,  
1086 Atmos. Chem. Phys., 9, 5131-5153, 2009.

1087 Zhang, Q., Zheng, Y., Tong, D., Shao, M., Wang, S., Zhang, Y., et al.: Drivers of  
1088 improved PM<sub>2.5</sub> air quality in China from 2013 to 2017. P. Natl. Acad. Sci., 116,  
1089 24463-24469, 2019.

1090 Zhang, X., Dai, H. C., Jin, Y. N., and Zhang, S. Q.: Evaluation of health and economic  
1091 benefits from “Coal to Electricity” Policy in the residential sector in the  
1092 Jing-Jin-Ji Region, Acta Scientiarum Naturalium Universitatis Pekinensis, 55, 2,  
1093 10.13209/j.0479-8023.2018.098, 2019 (in Chinese).

1094 Zhang, Y., Bo, X., Zhao, Y., and Nielsen, C. P.: Benefits of current and future policies  
1095 on emissions of China's coal-fired power sector indicated by continuous emission  
1096 monitoring, Environ. Pollut., 251, [415-424](#), 2019.

1097 Zhang, Y. H., Su, H., Zhong, L. J., Cheng, Y. F., Zeng, L. M., and Wang, X. S.:  
1098 Regional ozone pollution and observation-based approach for analyzing ozone-  
1099 precursor relationship during the PRIDE-PRD2004 campaign, Atmos. Environ.,  
1100 42, 6203-6218, 10.1016/j.atmosenv.2008.05.002, 2008.

1101 Zhao, B., Wang, S. X., Dong, X. Y., Wang, J. D., Duan, L., Fu, X., Hao, J. M., and Fu,  
1102 J.: Environmental effects of the recent emission changes in China: implications  
1103 for particulate matter pollution and soil acidification, Environ. Res. Lett., 8,  
1104 10.1088/1748-9326/8/2/024031, 2013.

1105 [Zhao, X., Zhao, Y., Chen, D., Li, C., and Zhang, J.: Top-down estimate of black](#)  
1106 [carbon emissions for city cluster using ground observations: A case study in](#)  
1107 [southern Jiangsu, China. Atmos. Chem. Phys., 19, 2095-2113,](#)  
1108 [10.5194/acp-19-2095-2019, 2019.](#)

1109 Zhao, Y., Zhang, J., and Nielsen, C. P.: The effects of recent control policies on trends  
1110 in emissions of anthropogenic atmospheric pollutants and CO<sub>2</sub> in China, Atmos.  
1111 Chem. Phys., 13, 487-508, 10.5194/acp-13-487-2013, 2013.

1112 Zhao, Y., Mao, P., Zhou, Y., Yang, Y., Zhang, J., Wang, S., Dong, Y., Xie, F., Yu, Y.,  
1113 and Li W.: Improved provincial emission inventory and speciation profiles of  
1114 anthropogenic non-methane volatile organic compounds: a case study for Jiangsu,  
1115 China, Atmos. Chem. Phys., 17, 7733-7756, 10.5194/acp-17-7733-2017, 2017.

1116 Zheng, B., Zhang, Q., Tong, D., Chen, C., Hong, C., Li, M., Geng, G., Lei, Y., Huo,  
1117 H., and He, K.: Resolution dependence of uncertainties in gridded emission

删除的内容: .

1119 inventories: a case study in Hebei, China, Atmos. Chem. Phys., 17, 921-933,  
1120 10.5194/acp-17-921-2017, 2017.  
1121 [Zheng, H., Zhao, B., Wang, S., Wang, T., Ding, D., Chang, X., Liu, K., and Xing, J.:](#)  
1122 [Transition in source contributions of PM2.5 exposure and associated premature](#)  
1123 [mortality in China during 2005-2015, Environ. Int. 132, 105111,](#)  
1124 [10.1016/j.envint.2019.105111, 2019.](#)  
1125 [Zhou, Y., Zhao, Y., Mao, P., Zhang, Q., Zhang, J., Qiu, L., and Yang, Y.:](#) Development  
1126 of a high-resolution emission inventory and its evaluation and application  
1127 through air quality modeling for Jiangsu Province, China, Atmos. Chem. Phys.,  
1128 17, 211-233, 10.5194/acp-17-211-2017, 2017.  
1129 ZJBS (Zhejiang Bureau of Statistics): Statistical Yearbook of Zhejiang, China  
1130 Statistics Press, Beijing, 2016 (in Chinese).  
1131

删除的内容: .



## 1133 **Figure captions**

1134 Figure 1. The modeling domain and the locations of the concerned provinces and their  
1135 capital cities. The numbers 1-4 represent the cities of Nanjing, Hefei, Shanghai and  
1136 Hangzhou, respectively. The map data provided by Resource and Environment Data  
1137 Cloud Platform are freely available for academic use  
1138 (<http://www.resdc.cn/data.aspx?DATAID=201>), © Institute of Geographic Sciences &  
1139 Natural Resources Research, Chinese Academy of Sciences.

1140 Figure 2. The spatial distributions of the simulated monthly SO<sub>2</sub>, NO<sub>2</sub>, O<sub>3</sub> and PM<sub>2.5</sub>  
1141 concentrations for Case 2 in D2 (unit: μg/m<sup>3</sup>).

1142 Figure 3. The spatial distributions of the relative changes (%) in the simulated  
1143 monthly SO<sub>2</sub>, NO<sub>2</sub>, O<sub>3</sub> and PM<sub>2.5</sub> concentrations between Cases 2 and 3 in D2 ((Case  
1144 [3-Case 2](#))/Case 2).

删除的内容: (Case 2-Case 3)

1145 Figure 4. The spatial distributions of the relative changes (%) in the simulated  
1146 monthly SO<sub>2</sub>, NO<sub>2</sub>, O<sub>3</sub> and PM<sub>2.5</sub> concentrations between Cases 2 and 4 in D2 ((Case  
1147 [4-Case 2](#))/Case 2).

删除的内容: (Case 2-Case 4)

1148 Figure 5. The spatial distributions of the annual PM<sub>2.5</sub> concentrations (average of  
1149 January, April, July and October) for Case 2 (a) and the reduced annual PM<sub>2.5</sub>  
1150 concentrations for Cases 3 (b) and 4 (c) in the YRD region (unit: μg/m<sup>3</sup>). Note the  
1151 different color ranges in the panels for easier visualization.

1152 Figure 6. The population fractions exposed to different levels of PM<sub>2.5</sub> in the YRD  
1153 region for Cases 2 (a), 3 (b), and 4 (c).

1154 Figure 7. The spatial distributions of the mortality (a) and YLL (b) attributable to  
1155 PM<sub>2.5</sub> exposure in Case 2 at a horizontal resolution of 9 km.

1156 Figure 8. Comparisons of the estimated mortality attributable to PM<sub>2.5</sub> exposure in  
1157 various studies for the YRD region.

1158 Figure 9. The spatial distributions of the avoided deaths and YLL attributable to the  
1159 reduced PM<sub>2.5</sub> exposure with ultra-low emission policy implementation at a horizontal  
1160 resolution of 9 km. Note the different color ranges in the panels for easier  
1161 visualization.

## Tables

**Table 1 The air pollutant emissions by sector for Cases 1-5 in YRD (Unit: Gg).**

Case	Power			Industry			Residential			Transportation			Total		
	SO <sub>2</sub>	NO <sub>x</sub>	PM	SO <sub>2</sub>	NO <sub>x</sub>	PM	SO <sub>2</sub>	NO <sub>x</sub>	PM	SO <sub>2</sub>	NO <sub>x</sub>	PM	SO <sub>2</sub>	NO <sub>x</sub>	PM
Case 1	606.8	863.4	376.2	1305.5	1294.6	1817.9	133.5	326.6	787.5	62.0	1847.1	105.9	2107.8	4331.7	3087.4
Case 2	179.4	245.5	45.1	1305.5	1294.6	1817.9	133.5	326.6	787.5	62.0	1847.1	105.9	1680.5	3713.8	2756.4
Case 3	56.0	110.0	8.8	1305.5	1294.6	1817.9	133.5	326.6	787.5	62.0	1847.1	105.9	1557.0	3578.4	2720.0
Case 4	56.0	110.0	8.8	249.4	426.8	539.6	133.5	326.6	787.5	62.0	1847.1	105.9	500.9	2710.6	1441.7
Case 5	0.0	0.0	0.0	1305.5	1294.6	1817.9	133.5	326.6	787.5	62.0	1847.1	105.9	1501.0	3468.4	2711.2

Note: Case 1: The emissions of coal-fired power sector were estimated based on the emission factor method without CEMS data. Case 2: The emissions of coal-fired power sector were estimated based on the improved method by Y. Zhang et al. (2019), with CEMS data incorporated. Case 3: All the coal-fired power plants in the YRD region were assumed to meet the requirement of the ultra-low emission policy. Case 4: All the coal-fired power plants and certain industrial sources including boilers, cement, and iron & steel factories in the YRD region were assumed to meet the requirement of the ultra-low emission policy. Case 5: The emissions of all coal-fired power plants were set at zero.

带格式的: 字体: 小四

带格式的: 字体: 小四

带格式的: 段落间距段前: 0.5 行

带格式的: 字体: 小四

带格式的: 字体: 小四

带格式的: 字体: 小四

带格式的: 字体: 小四

带格式的: 字体: 小四

带格式的: 字体: 小四

带格式的: 字体: 小四

带格式的: 字体: 小四

**Table 2 Comparison of the observed and simulated hourly SO<sub>2</sub>, NO<sub>2</sub>, O<sub>3</sub> and PM<sub>2.5</sub> concentrations by month for Cases 1 and 2 in the YRD region. Totally 230 state-operated observation sites were included in the comparison.**

删除的内容: s  
带格式的: 段落间距段后: 6 磅  
删除的内容: monthly  
删除的内容: in

Pollutant	R		NMB (%)		NME (%)		
	Case 1	Case 2	Case 1	Case 2	Case 1	Case 2	
SO <sub>2</sub>	Jan	0.72	0.89↑	11.44	0.52↑**	26.83	24.22↑
	Apr	0.36	0.45↑	-18.45	-22.62	31.65	34.81
	Jul	0.17	0.14	36.84	15.72↑***	58.69	48.44↑
	Oct	0.59	0.57	14.59	1.15↑***	32.49	29.22↑*
NO <sub>2</sub>	Jan	0.72	0.73↑	42.74	34.92↑*	44.25	37.88↑
	Apr	0.64	0.69↑	69.24	48.72↑***	70.24	51.81↑**
	Jul	0.71	0.71	145.42	131.65↑*	145.42	131.65↑*
	Oct	0.70	0.69	58.15	47.73↑*	58.86	49.41↑*
O <sub>3</sub>	Jan	0.74	0.75↑	-16.90	-6.40↑**	30.53	28.60↑
	Apr	0.78	0.67	-14.88	-9.89↑	23.14	27.48
	Jul	0.78	0.79↑	-34.49	-28.46↑	37.11	32.77↑
	Oct	0.80	0.78	-30.37	-28.28↑	34.32	33.60↑
PM <sub>2.5</sub>	Jan	0.89	0.90↑	-0.28	1.63	16.27	15.21↑
	Apr	0.76	0.76	9.94	2.57↑**	21.30	19.26↑
	Jul	0.64	0.63	30.44	24.08↑***	37.66	34.29↑*
	Oct	0.75	0.75	5.40	-11.80	23.34	22.28

Note: The arrows represent that the simulation in Case 2 were improved compared to Case 1. \*, \*\*, and \*\*\* indicate the improvements are statistically significant with confidence levels of 90%, 95%, and 99 %, respectively. The R, NMB and NME were calculated using the following equations ( $P$ ,  $O$ ,  $\bar{P}$ , and  $\bar{O}$  represent the simulation, observation, averaged simulation and averaged observation values, respectively):

删除的内容: s  
删除的内容: results

$$NMB = \frac{\sum_{i=1}^n (P_i - O_i)}{\sum_{i=1}^n O_i} \times 100\% \quad ; \quad NME = \frac{\sum_{i=1}^n |P_i - O_i|}{\sum_{i=1}^n O_i} \times 100\% \quad ;$$

$$R = \frac{\sum_{i=1}^n (P_i - \bar{P})(O_i - \bar{O})}{\sqrt{\sum_{i=1}^n (P_i - \bar{P})^2 \sum_{i=1}^n (O_i - \bar{O})^2}}$$

**Table 3 The relative (%) and absolute changes ( $\mu\text{g}/\text{m}^3$ , in parentheses) of the simulated monthly pollutant concentrations in different cases relative to Case 2 in the YRD region.**

Pollutant	(Case 3 - Case 2) / Case 2				(Case 4 - Case 2) / Case 2				(Case 5 - Case 2) / Case 2			
	Jan	Apr	Jul	Oct	Jan	Apr	Jul	Oct	Jan	Apr	Jul	Oct
SO <sub>2</sub>	-2.7	-4.8	-6.1	-4.3	-32.9	-57.3	-64.1	-55.1	-4.3	-11.4	-12.1	-12.1
	(-0.2)	(-0.2)	(-0.1)	(-0.2)	(-2.0)	(-1.8)	(-1.5)	(-2.4)	(-0.3)	(-0.4)	(-0.3)	(-0.5)
NO <sub>2</sub>	-2.0	-2.9	-2.0	-2.5	-16.4	-21.9	-17.1	-22.8	-2.6	-5.9	-4.1	-6.2
	(-0.4)	(-0.4)	(-0.3)	(-0.4)	(-3.2)	(-3.0)	(-2.5)	(-3.7)	(-0.5)	(-0.8)	(-0.6)	(-1.0)
O <sub>3</sub>	1.7	2.2	0.8	2.2	10.4	9.7	2.6	14.0	-2.0	2.7	-1.6	4.5
	(0.4)	(0.9)	(0.3)	(0.8)	(2.6)	(4.1)	(0.8)	(4.8)	(-0.5)	(1.2)	(-0.5)	(1.5)
PM <sub>2.5</sub>	-0.1	-0.5	-1.3	-0.5	-6.2	-14.6	-21.6	-14.3	-1.7	-2.4	-4.3	-0.9
	(-0.1)	(-0.2)	(-0.4)	(-0.2)	(-4.6)	(-6.0)	(-6.5)	(-6.3)	(-1.3)	(-1.0)	(-1.3)	(-0.4)

**Table 4 The estimated mortality and YLL attributable to PM<sub>2.5</sub> exposures in Case 2 over the YRD region.**

	<b>STK</b>	<b>IHD</b>	<b>COPD</b>	<b>LC</b>	<b>LRI</b>	<b>Total</b>
<b>Deaths (<math>\times 10^3</math> person)</b>						
Anhui	19.6 (10.7-29.0)	19.1 (11.0-29.8)	15.2 (9.8-21.0)	8.0 (5.5-10.3)	3.1 (2.4-3.8)	65.0 (39.4-93.9)
Shanghai	4.3 (2.3-6.5)	4.2 (2.4-6.6)	4.4 (2.7-6.1)	2.6 (1.7-3.3)	0.8 (0.6-1.0)	16.3 (9.8-23.4)
Jiangsu	23.6 (12.7-35.0)	31.3 (17.8-48.8)	12.8 (8.1-17.7)	8.1 (5.5-10.5)	3.7 (2.8-4.5)	79.5 (46.8-116.5)
Zhejiang	8.7 (4.2-13.4)	6.8 (3.6-10.4)	10.8 (6.2-15.4)	5.0 (3.1-6.9)	1.6 (1.1-2.0)	32.9 (18.2-48.2)
YRD	56.2 (29.9-83.8)	61.4 (34.7-95.5)	43.3 (26.8-60.2)	23.6 (15.8-31.0)	9.2 (7.0-11.3)	193.8 (114.2-281.9)
<b>YLL (<math>\times 10^4</math> year)</b>						
Anhui	30.1 (16.6-44.0)	29.6 (17.3-45.6)	66.0 (42.3-91.1)	34.5 (23.7-44.4)	13.6 (10.4-16.4)	173.7 (110.3-241.5)
Shanghai	6.7 (3.6-9.8)	6.5 (3.8-10.0)	19.0 (11.9-26.2)	11.0 (7.4-14.4)	3.5 (2.7-4.3)	46.7 (29.4-64.8)
Jiangsu	36.2 (19.7-53.1)	48.6 (28.0-74.7)	55.6 (35.0-76.7)	35.0 (23.6-45.6)	16.0 (12.3-19.4)	191.4 (118.5-269.5)
Zhejiang	13.3 (6.5-20.5)	10.6 (5.7-16.0)	46.9 (26.7-66.6)	21.8 (13.6-30.0)	6.8 (4.8-8.9)	99.4 (57.2-141.9)
YRD	86.3 (46.3-127.4)	95.3 (54.7-146.4)	187.4 (115.9-260.6)	102.3 (68.3-134.4)	40.0 (30.1-48.9)	511.3 (315.5-717.7)

**Table 5 The reduced attributable deaths (person) and rates (in parentheses) resulting from implementation of the ultra-low emission policy in the YRD region.**

	<b>STK</b>	<b>IHD</b>	<b>COPD</b>	<b>LC</b>	<b>LRI</b>	<b>Total</b>
<b>Case 3</b>						
Anhui	26 (0.13%)	19 (0.10%)	24 (0.16%)	18 (0.22%)	6 (0.18%)	92 (0.14%)
Shanghai	1 (0.03%)	1 (0.02%)	1 (0.03%)	1 (0.04%)	0 (0.04%)	5 (0.03%)
Jiangsu	51 (0.22%)	51 (0.16%)	34 (0.27%)	30 (0.37%)	11 (0.31%)	177 (0.22%)
Zhejiang	7 (0.08%)	4 (0.06%)	11 (0.10%)	7 (0.14%)	2 (0.13%)	31 (0.10%)
YRD	85 (0.15%)	74 (0.12%)	71 (0.16%)	55 (0.23%)	19 (0.21%)	305 (0.16%)
<b>Case 4</b>						
Anhui	901 (4.59%)	650 (3.41%)	848 (5.56%)	605 (7.60%)	196 (6.23%)	3200 (4.92%)
Shanghai	281 (6.46%)	204 (4.84%)	348 (7.95%)	277 (10.86%)	75 (9.20%)	1185 (7.26%)
Jiangsu	1192 (5.05%)	1179 (3.76%)	794 (6.19%)	684 (8.47%)	264 (7.14%)	4114 (5.17%)
Zhejiang	475 (5.49%)	283 (4.16%)	765 (7.06%)	491 (9.77%)	138 (8.72%)	2152 (6.54%)
YRD	2848 (5.06%)	2316 (3.77%)	2755 (6.37%)	2058 (8.71%)	673 (7.28%)	10651 (5.50%)

**Table 6 The reduced cases and rates (in parentheses) of YLL resulting from implementation of the ultra-low emission policy in the YRD region.**

	STK	IHD	COPD	LC	LRI	Total
Case 3						
Anhui	396 (0.13%)	285 (0.10%)	1058 (0.16%)	760 (0.22%)	243 (0.18%)	2743 (0.16%)
Shanghai	17 (0.03%)	13 (0.02%)	60 (0.03%)	45 (0.04%)	13 (0.04%)	148 (0.03%)
Jiangsu	783 (0.22%)	774 (0.16%)	1480 (0.27%)	1282 (0.37%)	491 (0.31%)	4809 (0.25%)
Zhejiang	107 (0.08%)	66 (0.06%)	483 (0.10%)	301 (0.14%)	87 (0.13%)	1044 (0.11%)
YRD	1303 (0.15%)	1138 (0.12%)	3118 (0.16%)	2388 (0.23%)	834 (0.21%)	8744 (0.17%)
Case 4						
Anhui	13733 (4.56%)	9946 (3.36%)	36709 (5.56%)	26218 (7.60%)	8480 (6.23%)	95086 (5.47%)
Shanghai	4284 (6.43%)	3127 (4.78%)	15083 (7.95%)	11993 (10.86%)	3233 (9.20%)	37719 (8.07%)
Jiangsu	18192 (5.02%)	18066 (3.72%)	34393 (6.19%)	29638 (8.47%)	11451 (7.14%)	111740 (5.84%)
Zhejiang	7297 (5.49%)	4380 (4.13%)	33115 (7.06%)	21255 (9.77%)	5972 (8.72%)	72018 (7.25%)
YRD	43506 (5.04%)	35518 (3.73%)	119300 (6.37%)	89104 (8.71%)	29135 (7.28%)	316562 (6.19%)

Figure 1

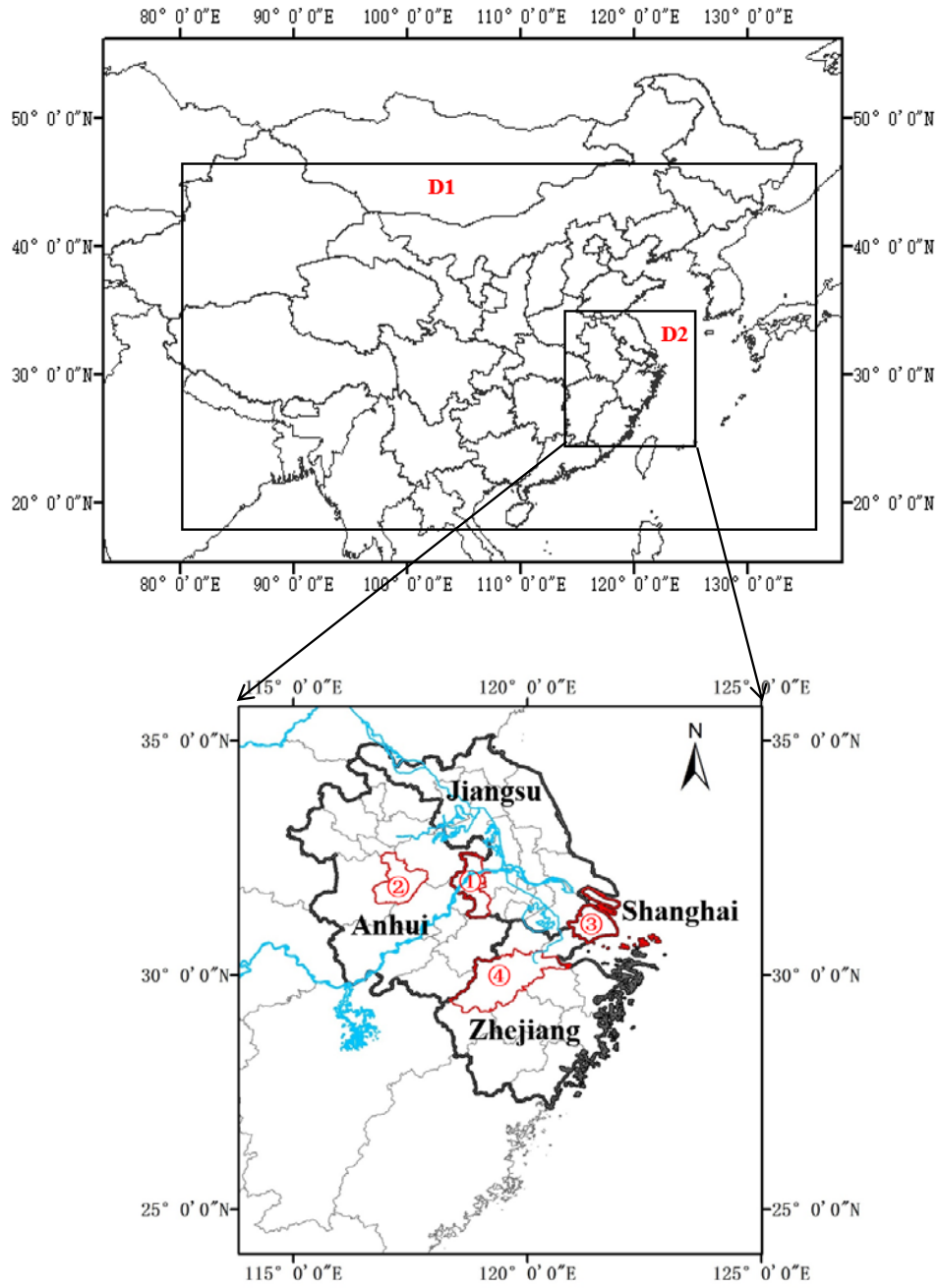




Figure 2

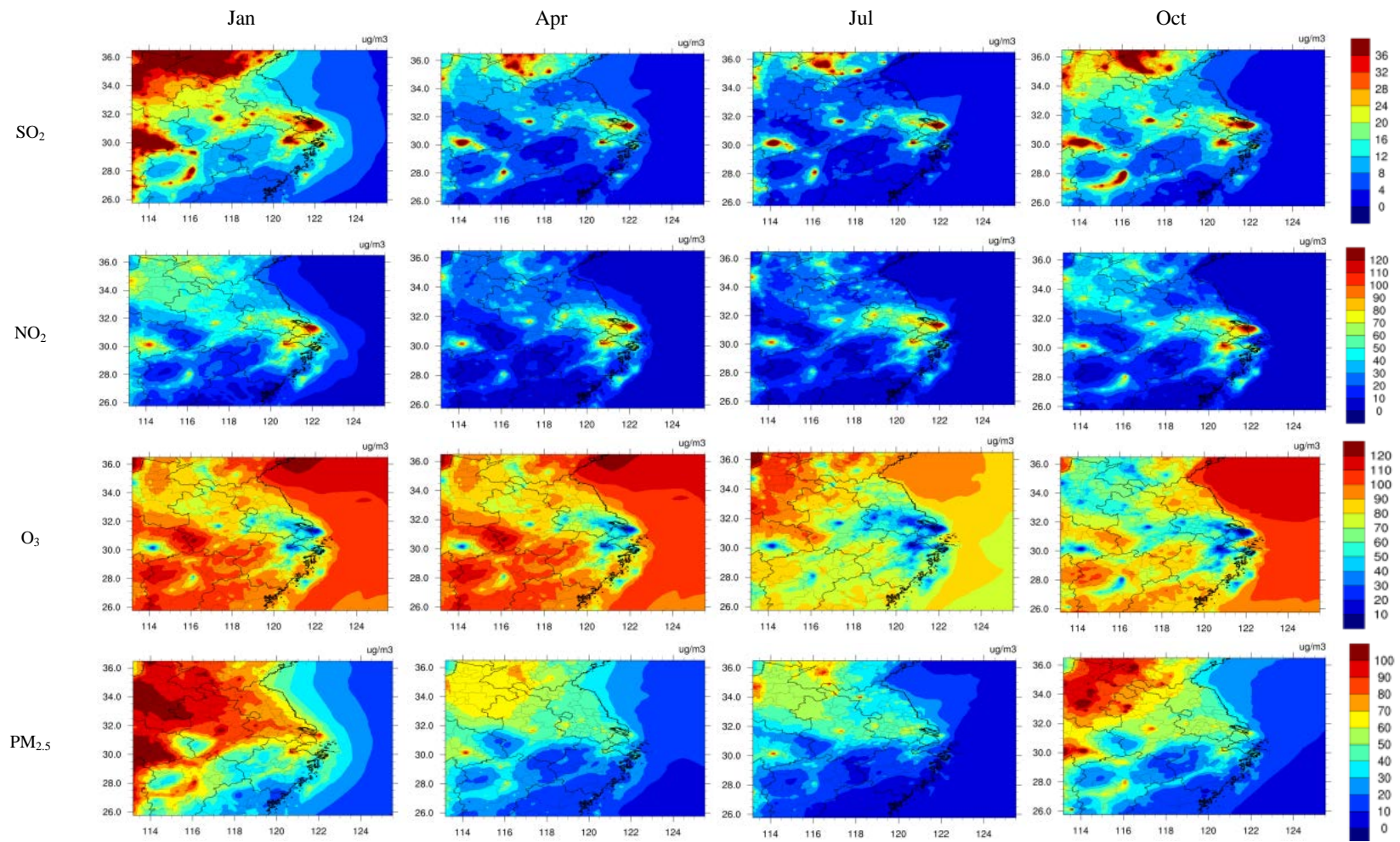


Figure 3

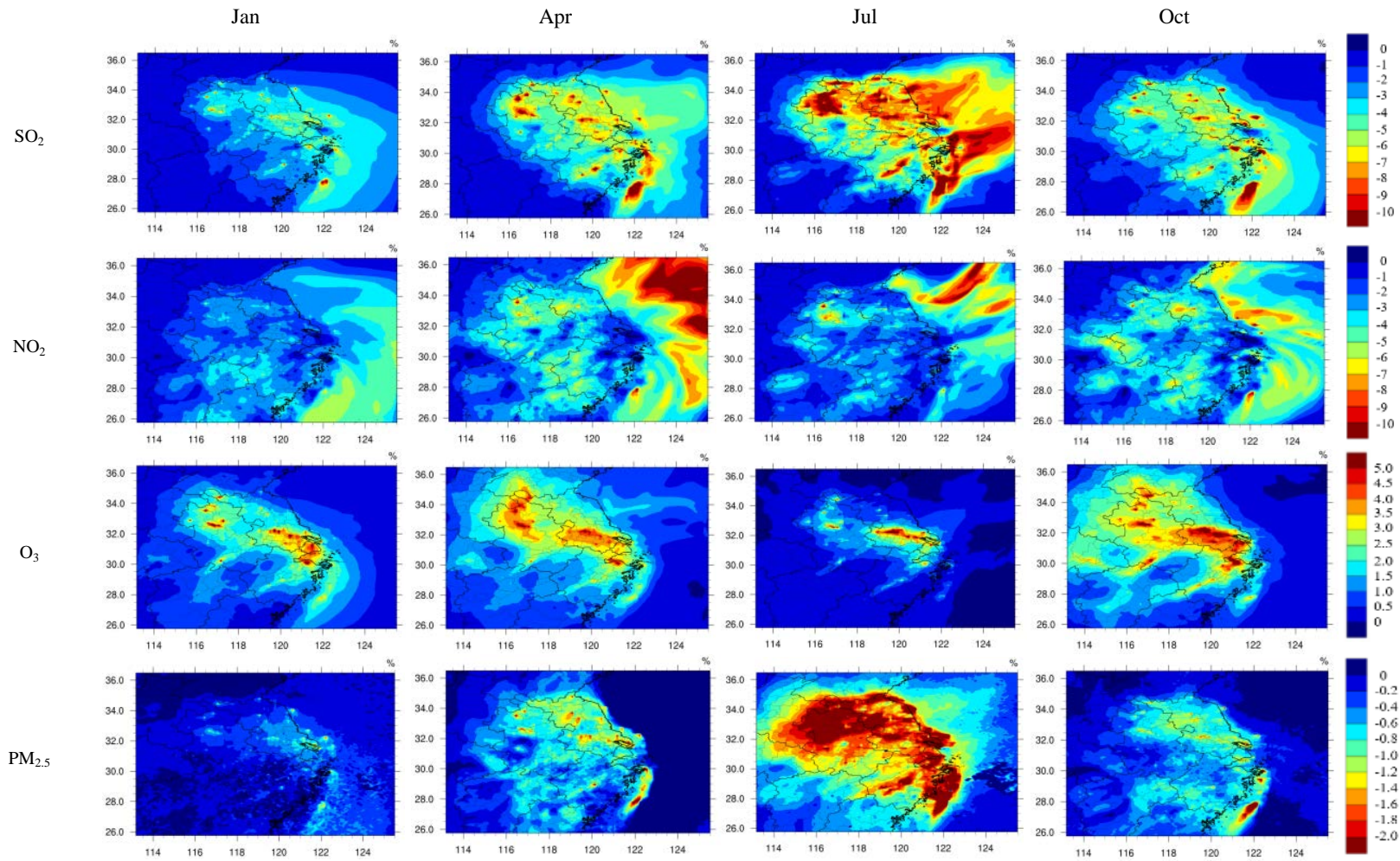


Figure 4

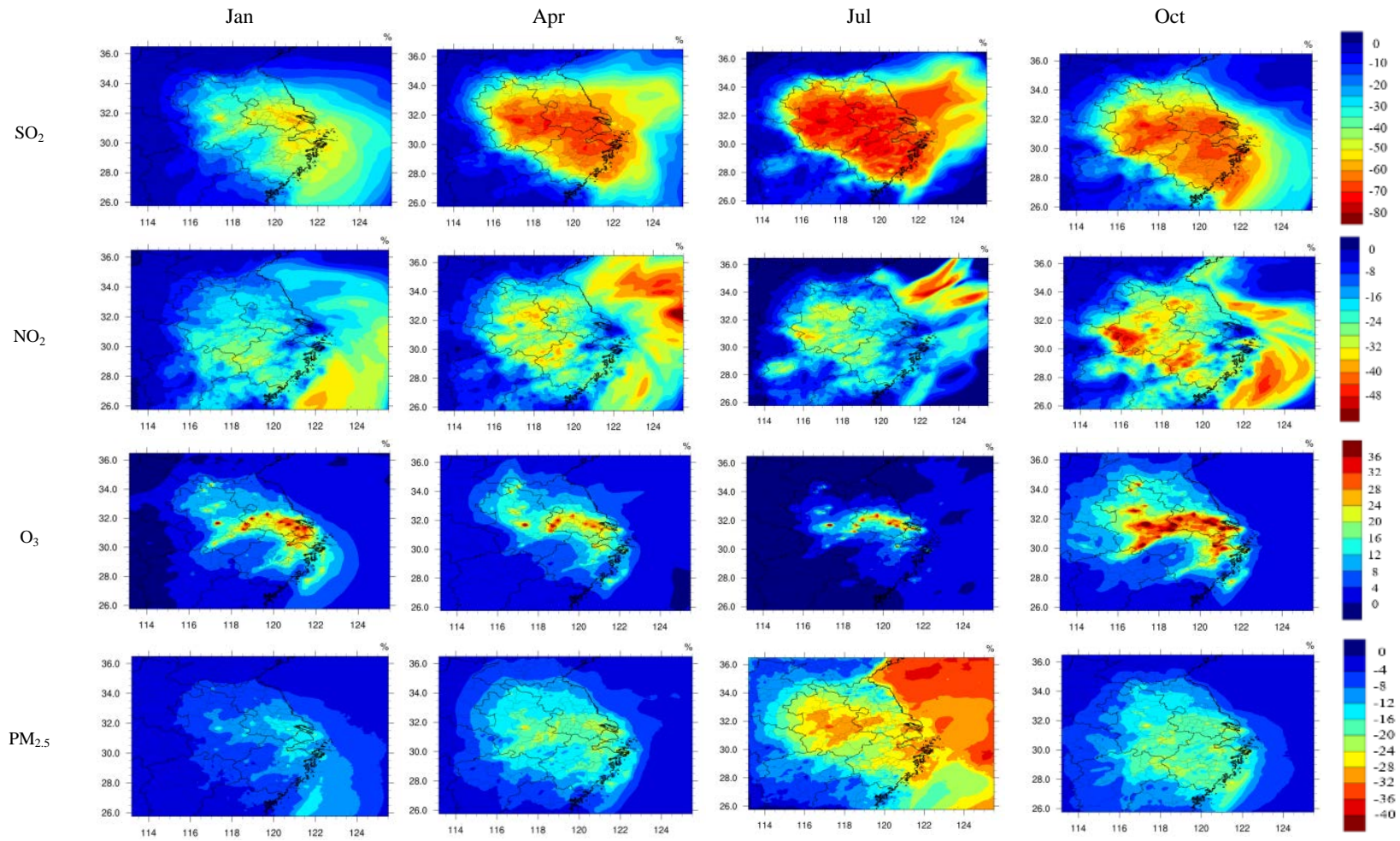
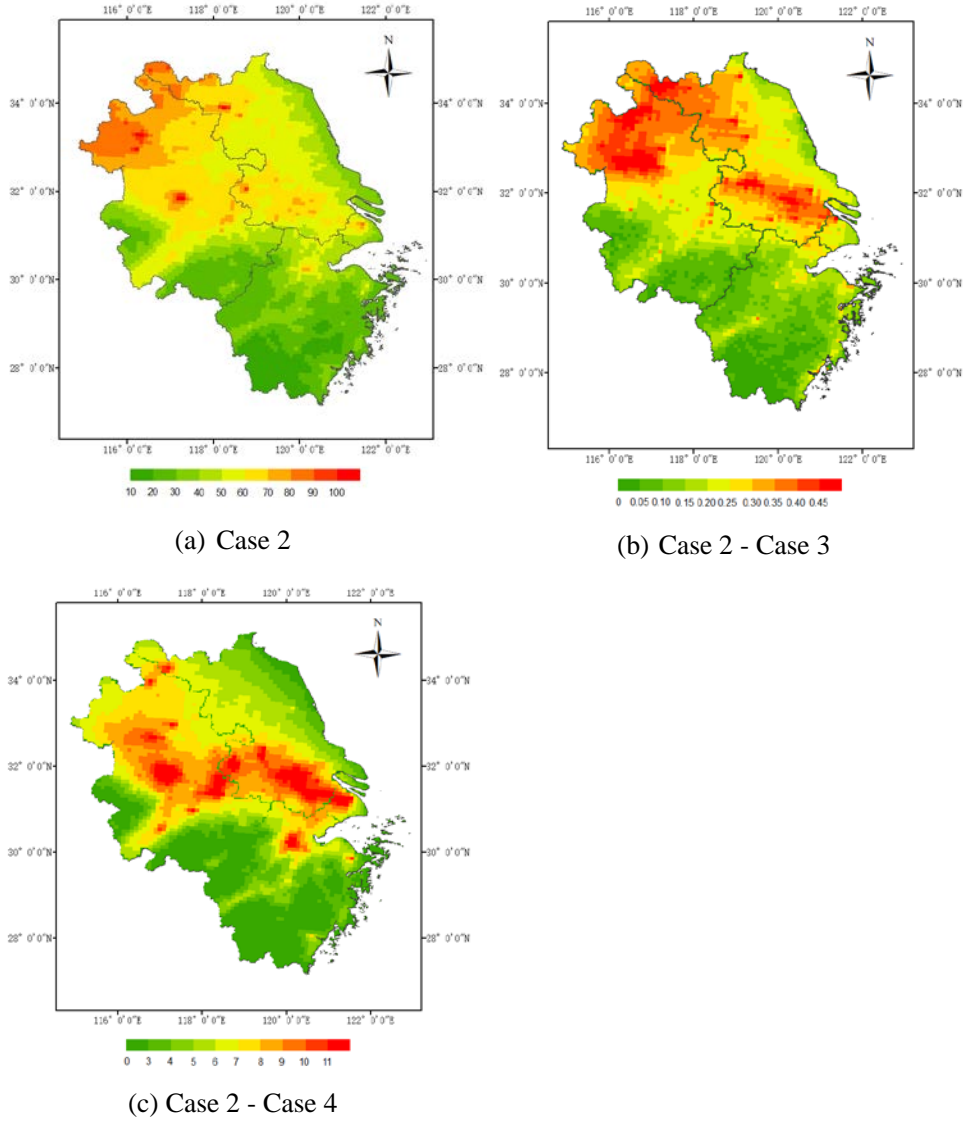
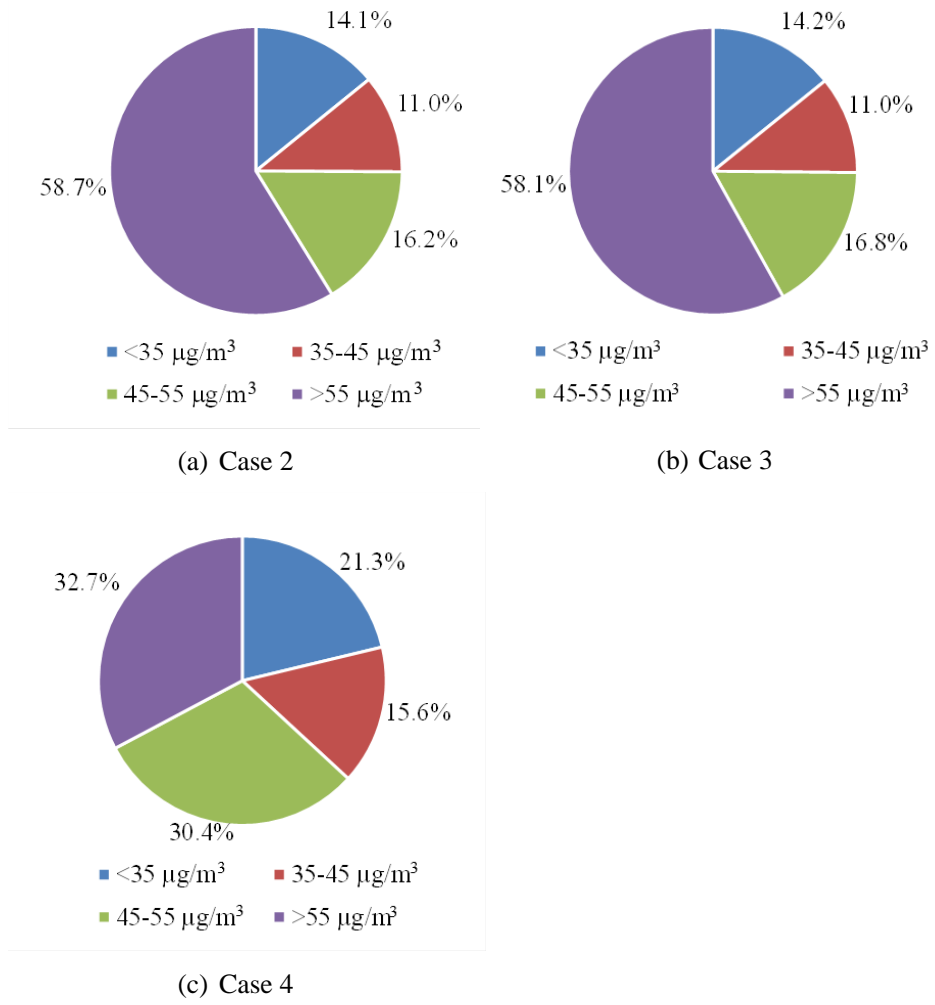


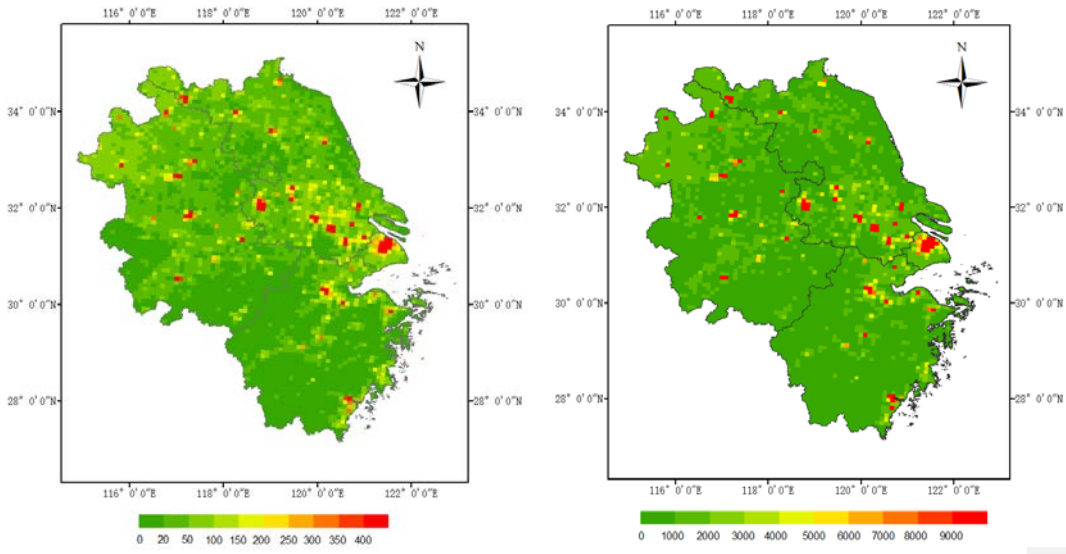
Figure 5



**Figure 6**



**Figure 7**



(a) Deaths (unit: person)

(b) YLL (unit: year)

**Figure 8**

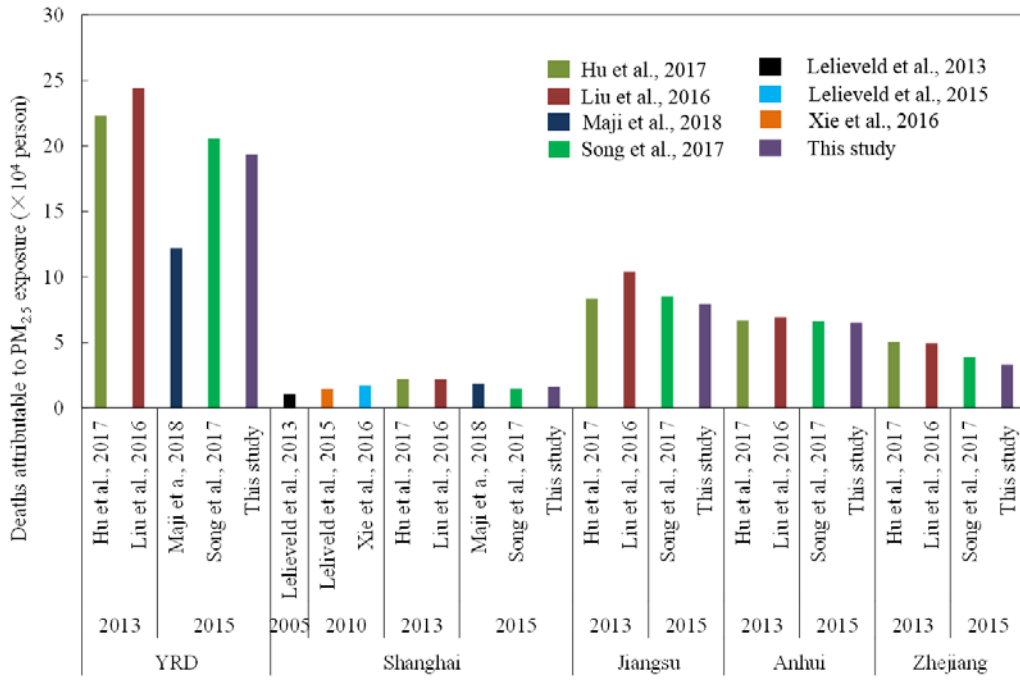
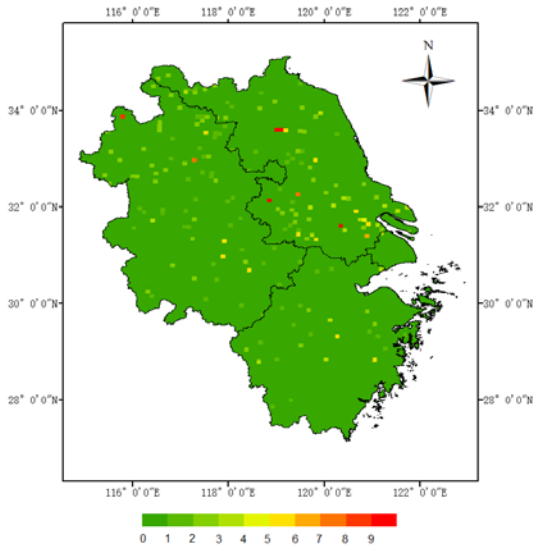
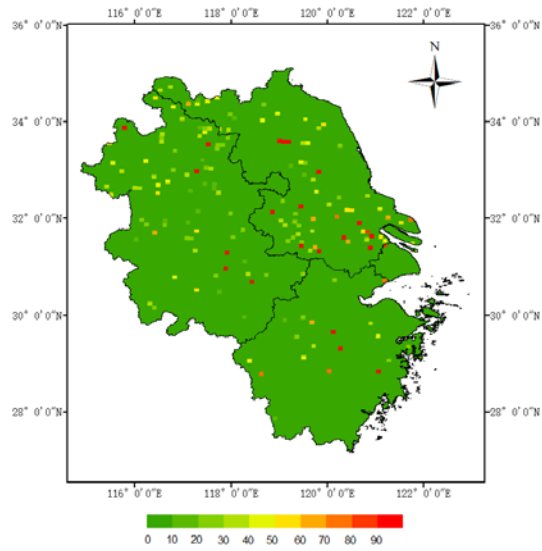


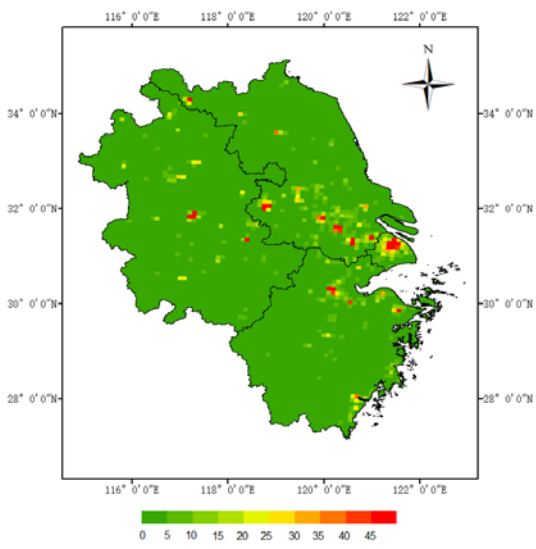
**Figure 9**



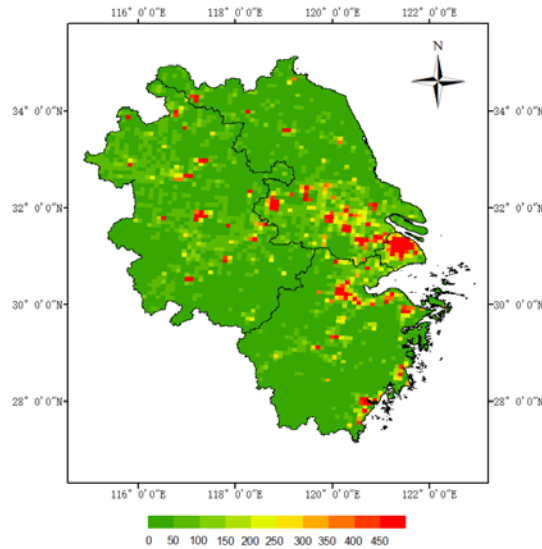
(a) Avoided deaths in Case 3 (unit: person)



(b) Avoided YLL in Case 3 (unit: year)



(c) Avoided deaths in Case 4 (unit: person)



(d) Avoided YLL in Case 4 (unit: year)